BBC

ENGINEERING DIVISION

MONOGRAPH

The non-linear characteristics of klystron amplifiers

by

D. J. WHYTHE, B.Sc.(Eng.), M.I.E.E.

J. L. EATON, B.Sc., M.I.E.E.

(Research Department, BBC Engineering Division)

BBC ENGINEERING MONOGRAPH

No. 74

THE NON-LINEAR CHARACTERISTICS OF
KLYSTRON AMPLIFIERS

by

D. J. Whythe, B.Sc.(Eng.), M.I.E.E.

J. L. Eaton, B.Sc., M.I.E.E.

(Research Department, BBC Engineering Division)

JUNE 1968

BRITISH BROADCASTING CORPORATION

FOREWORD

THIS is one of a series of Engineering Monographs published by the British Broadcasting Corporation. About six are produced every year, each dealing with a technical subject within the field of television and sound broadcasting. Each Monograph describes work that has been done by the Engineering Division of the BBC and includes, where appropriate, a survey of earlier work on the same subject. From time to time the series may include selected reprints of articles by BBC authors that have appeared in technical journals. Papers dealing with general engineering developments in broadcasting may also be included occasionally.

This series should be of interest and value to engineers engaged in the fields of broadcasting and of telecommunications generally.

Individual copies cost 5s. post free, while the annual subscription is £1 post free. Orders can be placed with newsagents and booksellers, or BBC PUBLICATIONS, 35 MARYLEBONE HIGH STREET, LONDON, W.1.

CONTENTS

PREVIOUS ISSUES IN THIS SERIES

THE NON-LINEAR CHARACTERISTICS OF KLYSTRON AMPLIFIERS

SUMMARY

A method is shown by which the two-cavity ballistic theory of klystrons may be extended to apply to four-cavity klystrons used for television broadcasting. Measured distortions of television signals, and measured levels of harmonics and intermodulation products, occurring in a typical four-cavity klystron are shown to be in good agreement with calculated values. It is concluded that the non-linear characteristics of klystron amplifiers are largely fundamental to their mode of operation.

1. Introduction

Klystron amplifiers are used extensively at the present time as the output stage of Band IV/V (470 to 960 MHz) transmitters. The stations at which they are used can be classed into two groups: high-power stations where separate klystrons are used for the sound and vision signals, and translator stations where a single klystron handles the modulated luminance, chrominance, and sound signals simultaneously. Klystron amplifiers have a non-linear transfer characteristic which presents difficulties at both types of station but the difficulties are particularly severe at translator stations, where the effect is to generate in-band intermodulation products, which cause bar-patterns on the received pictures. At the present time, such bar-patterns can be reduced to a sufficiently low level only by drastically under-running the klystron, at the consequent expense of efficiency. At high-power stations, where separate klystrons are used for the sound and vision signals, the non-linear transfer characteristic is manifest mainly by the differential amplitude distortion which it causes on the transmitted signal, and by the high levels of harmonics and out-of-band intermodulation products which impose severe high-power filtering problems at certain stations.

It has therefore become important to assess the degree of non-linearity which is fundamental to the klystron operation and hence to appreciate the best possible performance that can be expected. The theory of the klystron amplifier, however, is quite involved. Several theories have been suggested over the past thirty years, but they all rely on various approximations and assumptions. In the main, they set out to define only the primary characteristics of the klystron, such as gain, bandwidth, and efficiency; only one theory deals with its non-linear characteristics. This theory, upon which the content of this monograph is based, was first applied to calculate harmonic levels but, more recently, it has been extended to include the levels of intermodulation products. All these theories are reasonably straightforward when applied to the simple case of a two-cavity klystron, but they become impracticable when applied to four-cavity klystrons of the type used for television broadcasting. Furthermore, surprisingly little has been published to show the agreement between theoretical and measured results, even for two-cavity klystrons.

This monograph describes further work which was carried out to adapt the existing theories to four-cavity klystrons used for television broadcasting. It shows how a four-cavity klystron can be represented by a two-cavity model and how the existing theories can be applied to calculate not only the levels of harmonics and intermodulation products but also the degree of amplitude and phase distortion. Measured results are shown to be in good general agreement with these theoretical predictions and it is concluded that the non-linear behaviour of the klystron is largely fundamental to its mode of operation.

2. Theory of the Klystron Amplifier

2.1 General Principle

The klystron is one of a class of high-frequency valves that amplify by a process termed 'velocity modulation'. As distinct from a conventional valve in which the flow of electrons is varied according to the instantaneous amplitude of the input signal (density modulation), a constant flow of electrons leaves the cathode of a velocity-modulated valve. The input signal causes some electrons to travel faster than others towards the anode (or 'collector'); the electrons therefore form 'bunches' and the beam becomes density-modulated upon arrival at the output terminals.
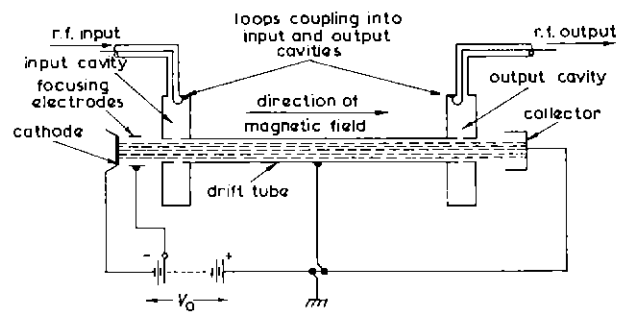
Fig. 1 — Two-cavity klystron

Fig. 1 shows a two-cavity klystron in diagrammatic form. A uniform stream of electrons leaving the cathode is electrostatically focused into a cylindrical beam and accelerated towards the input cavity by the applied voltage V_0. The velocity with which electrons enter this input cavity is given by

$$u_0 = (2\eta V_0)^{\frac{1}{2}} \qquad (1)$$

where η is the electron charge/mass ratio ($1 \cdot 76 \times 10^{11}$ coulomb/kg).* Since V_0 is usually about 10 kV, u_0 is

* This neglects relativistic effects. For the velocities in question the error introduced is $1 \cdot 5$ per cent.

typically about one-fifth the velocity of light. After passing through the input cavity, the electrons flow with constant velocity through a field-free region (termed the 'drift tube') before passing through the output cavity and arriving at the collector. Over this region, the electron focusing is maintained by a longitudinal magnetic field and, if no signal is applied to the input cavity, it follows that the electrons pass through both cavities and the drift tube with constant velocity u_0. For convenience, the two cavities and the drift tube are earthed. The magnetic focusing system is designed for minimum current to flow to these earthy parts (or 'body') of the valve; the 'body current' is typically less than 1 per cent of the collector current.

When a signal is applied to the input cavity a transverse alternating electric field occurs across the cavity in the direction of flow of the beam electrons; its effect is to cause those electrons which pass through the input cavity during positive half-cycles to travel in the drift tube with velocity greater than u_0 and those which pass through during negative half-cycles to travel in the drift tube with velocity less than u_0. The result is shown by means of the Applegate diagram drawn in Fig. 2 in which the positions of electrons along the drift tube are plotted against time. Suppose the effect of the alternating electric field across the input cavity is to superimpose a small sinusoidal variation of velocity upon the mean velocity u_0, as shown in the lower part of Fig. 2. Since each electron travels along the drift tube with constant velocity, the paths of all electrons can be represented by straight lines but the slopes of the lines will be greater or less than the mean slope, depending upon the velocity with which each electron leaves the input cavity. Fast electrons catch up with (and overtake) the slower electrons such that 'bunches' form along the drift tube with period equal to that of the input signal; there is clearly an optimum position for the output cavity where the bunching is greatest, corresponding roughly to S_2 in Fig. 2. At S_1 the bunching has not fully developed, whilst at S_3 the fast electrons have well overtaken the slow ones and the bunching has decreased.

The current passing through the output cavity has a waveform that is rich in harmonics; for optimum gain, output power and efficiency, the output cavity is positioned where the fundamental component of the current is a maximum. For a given beam current and velocity (i.e. a given beam power) there is a maximum power (the 'saturated' power) that can be delivered to the output cavity, occurring when the beam is optimally bunched as it passes through. If the input power is further increased, the output power decreases.

Theories describing this bunching action fall into two classes: ballistic theories based on the Applegate diagram[1,2] and plasma theories[3,4,5] which employ a linear wave equation to describe propagation along the beam; empirical formulae have also been proposed which attempt to combine the two classes.[6] A helpful comparison of the various theories is given by Sims and Stephenson[7] who show that the plasma and ballistic theories agree at low signal levels. The plasma theories break down, how-
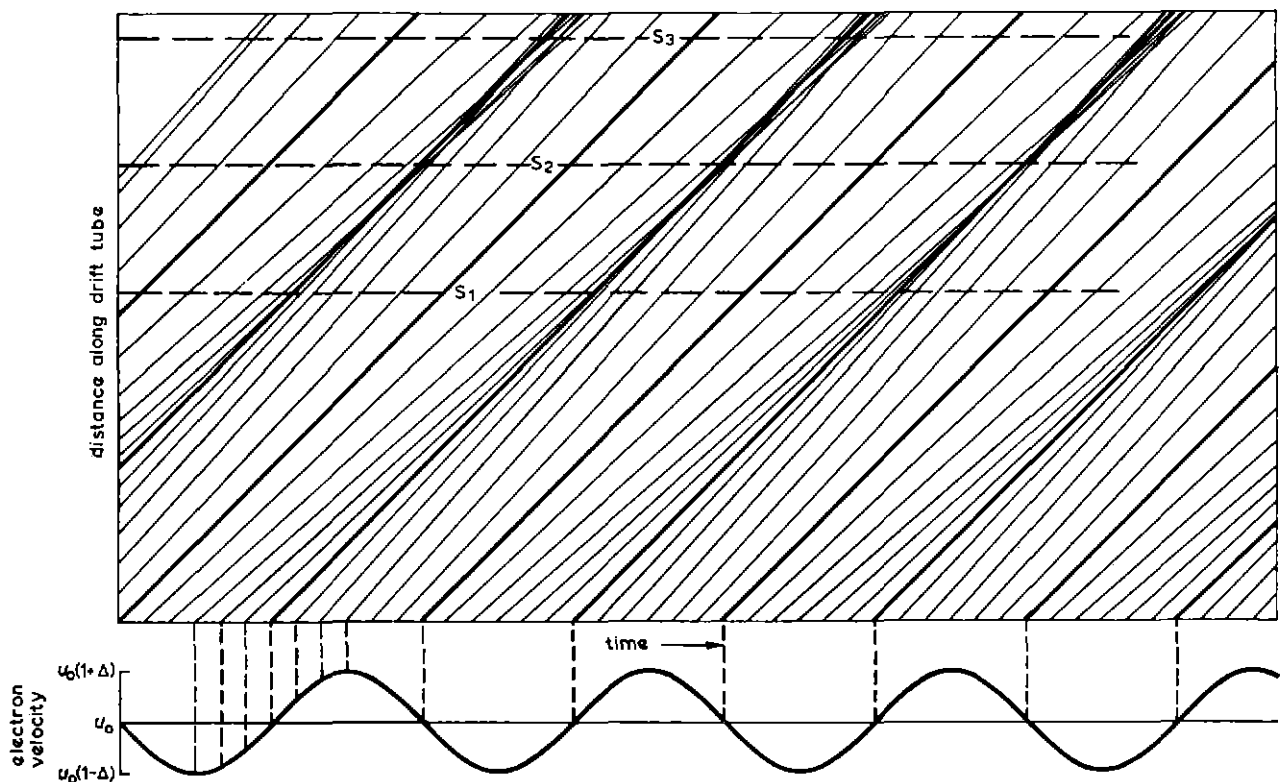
Fig. 2 — Applegate diagram showing the travel of electrons along the drift tube

6

ever, when the input signal is large enough to cause electron overtaking in the drift tube and thus, because that is the condition in which high-power klystrons are operated, only the ballistic theory is considered in this report.

2.2 The Ballistic Theory of Two-cavity Klystrons
2.2.1 Sinusoidal Input Signal

The first theory of klystrons, developed by Webster,[1] was a ballistic theory in which each electron in the beam was considered to travel throughout the drift tube with constant velocity. This is satisfactory for small signals but, when the electrons form into bunches, mutual repulsion between the electrons cannot be neglected. Webster[1] derived a first-order 'de-bunching' correction to allow for this effect but, as will be shown, this is not important when considering the non-linear performance. The ballistic theory is given in the Appendix (Section 10.1); it is convenient to discuss here the approximations involved and the results obtained.

If a sinusoidal input signal $V_1 \sin \omega t$ is applied across the input cavity, an electron that leaves the input cavity at time t does so with a velocity given approximately by

$$u = u_0(1 + \Delta \sin \omega t) \qquad (2)$$

where

$$\Delta = \frac{\xi V_1}{2V_0}$$

and ξ is a gap-coupling factor which depends upon the geometry of the gap and the beam.

This assumes Δ to be much less than unity and, even in high-power klystrons, this is a valid approximation. It also assumes that the time taken for an electron to pass across the gap of the input cavity is negligibly small compared to the period of the input signal, $2\pi/\omega$. This also is justifiable because the transit time across the gap occupies only about 1 per cent of the signal period at 500 MHz. For a two-cavity klystron, the factor ξ is unimportant because it affects only the gain of the tube, not its non-linear characteristics. It is an important factor, however, when applied to the intermediate cavities of a multi-cavity klystron (see Section 2.3) because it determines to what extent they influence the bunching of the beam and hence both the gain and the non-linearity of the tube.

It is evident from Fig. 2 that the degree of bunching on the beam as it passes through the output cavity will depend upon the amplitude of the input signal and upon the distance z between the two cavities. As shown in the Appendix (Section 10.1) the bunching also depends equally upon the values of ω and u_0; it is therefore convenient to use a 'bunching parameter' K given by

$$K = \frac{\omega z \Delta}{u_0} \qquad (3)$$

to define the bunching on the beam as it passes through the output cavity. The waveform of the beam current
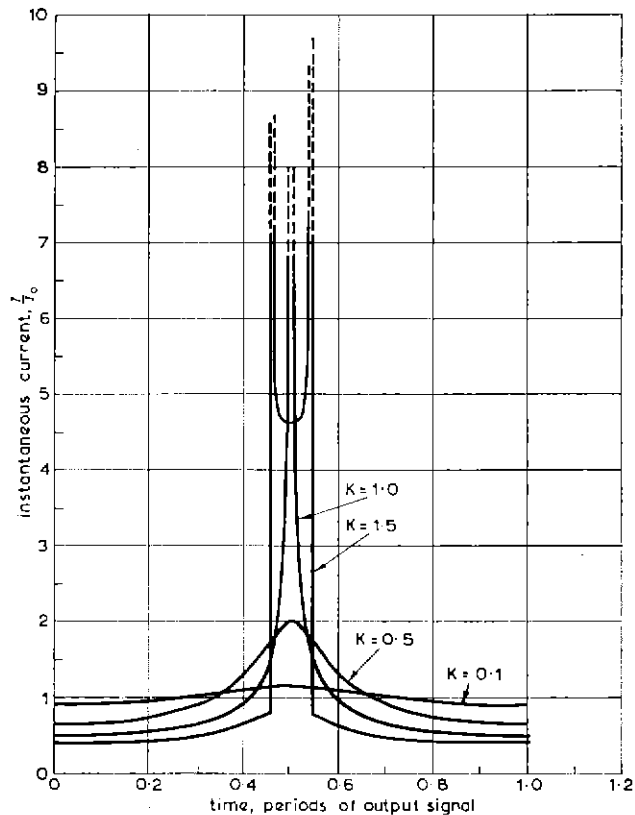
Fig. 3 — Waveform of current entering output cavity of two-cavity klystron

entering the output cavity is shown for various values of K in Fig. 3. When K is small the variation of current is small and approximately sinusoidal but, as K increases to a value equal to or greater than unity, the waveform develops infinite peaks which are rich in harmonics. These infinite peaks occur at the instants when electrons overtake on entering the output cavity. If $K = 1$, overtaking occurs once during each r.f. cycle; if $K > 1$, overtaking occurs more than once during each cycle whilst, if $K < 1$, overtaking does not occur at all. As shown in the Appendix (Section 10.1), the output voltage may be expressed as a series of harmonic terms given by

$$V_{\text{out}} = aI_0\left[1 + 2\sum_{r=1}^{\infty} F_r J_r(rK) \cos (r\omega t)\right] \qquad (4)$$

where F_r is a factor determined by the amplitude/frequency characteristic of the output cavity, a is a constant proportional to the product of the input and output gap coupling factors, and $J_r(rK)$ is the Bessel function of the first kind of order r and argument rK.

It would appear from Equation (3) that the bunching parameter (and hence the gain of the tube) can be increased without limit by making the drift tube long enough. As Webster has shown,[1] however, the effect of de-bunching modifies the value of K such that, for small signals, it becomes

7

$$K' = K\frac{\sin (hz)}{hz}$$

where h is a factor depending upon the current density of the beam. The optimum value of z (i.e. $\pi/2h$) is equal to one-quarter plasma-wavelength, a result also given by the plasma theories. This particular correction for de-bunching is a function only of the beam current and the design of the drift tube. It is therefore useful to the klystron designer in that it determines the optimum drift tube length but it does not affect the linear dependence of the bunching parameter upon the amplitude of the input signal. This is clearly an approximation and, on physical grounds, it is evident that the general effect of de-bunching is to 'soften' the current waveform, rounding off the infinite peaks of current. Whilst de-bunching would therefore be expected to have a significant effect upon the levels of high-order harmonics and intermodulation products, it can be neglected where, as in this monograph, only low-order non-linear products are being considered. It will later be shown that the simple ballistic theory, neglecting de-bunching entirely, agrees well with experiment for power levels up to about half the saturated power—disparities between theory and practice at the higher power levels could possibly be traced partly to de-bunching effects.
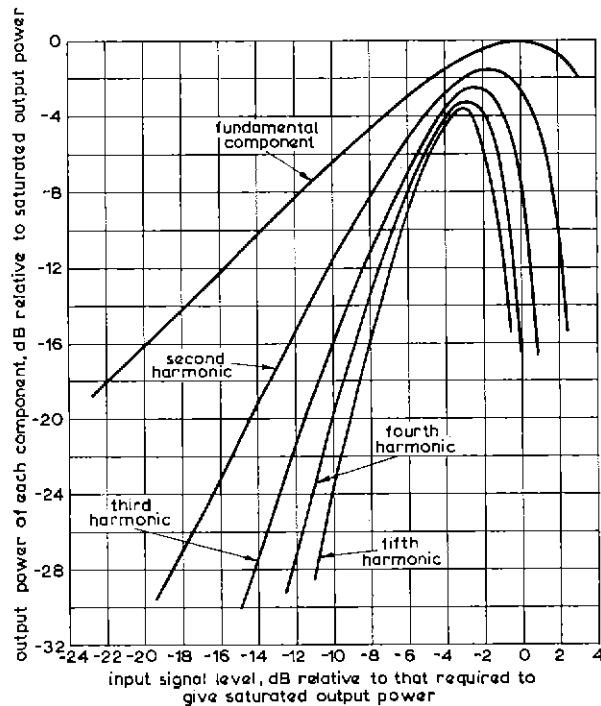
Fig. 4 — Theoretical harmonic levels in a two-cavity klystron

Fig. 4 shows the theoretical variation of output power at the fundamental and harmonic frequencies, as a function of input signal amplitude, calculated from Equation (4), neglecting the selectivity of the output cavity at the harmonic frequencies. The extreme non-linearity of the klystron is evident; at a power level slightly less than the

saturated power, the level of the second harmonic component of the beam is only -1 dB relative to that of the fundamental component.

When the klystron is delivering its saturated power, the peak value of the fundamental component of beam current is $1 \cdot 16$ times the mean beam current. If it is assumed that the output voltage cannot exceed the beam voltage (i.e. that from cathode to body), the maximum theoretical efficiency is given by $1 \cdot 16/2$ or 58 per cent; as will be shown, the efficiency obtained in practice is often very much less.

2.2.2 Modulated Input Signal

By extending Webster's theory to include input signals which comprise three sinusoidal signals applied simultaneously, Murata[8] has shown that the level of each harmonic or intermodulation product in the bunched beam is proportional to

$$a_{mnp} = J_m(\alpha) \cdot J_n(\beta) \cdot J_p(\gamma) \qquad (5)$$

In Equation (5) the integers m, n, p (positive or negative) represent the order of the intermodulation term. If, for example, input signals at frequencies f_1, f_2, f_3 are applied simultaneously, Equation (5) gives the level of the component at frequency $(mf_1 + nf_2 + pf_3)$. The parameters α, β, γ are given by

$$\alpha = K_1(mf_1 + nf_2 + pf_3)/f_1$$
$$\beta = K_2(mf_1 + nf_2 + pf_3)/f_2 \qquad (6)$$
$$\gamma = K_3(mf_1 + nf_2 + pf_3)/f_3$$

where K_1, K_2, K_3 are the bunching parameters of the beam (as defined by Webster, with or without a correction for de-bunching) which would apply if each of the input signals at f_1, f_2 and f_3 respectively were applied in the absence of the other two. If the only input signal is that at frequency f_1, $K_2 = K_3 = n = p = 0$ in Equation (6). Equation (5) then reduces to

$$a_{moo} = J_m(mK_1)$$

which corresponds to Equation (4).

These expressions will be used extensively in Section 4.
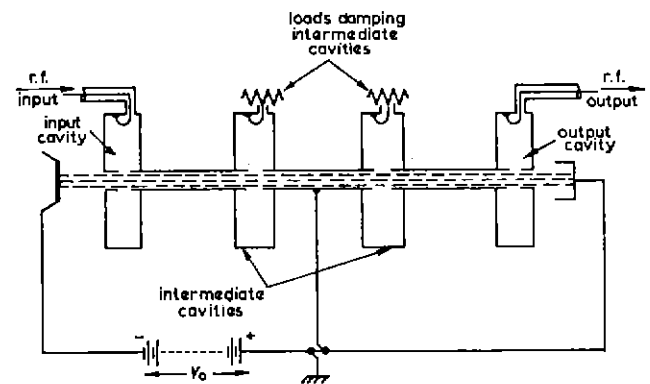
Fig. 5 — Four-cavity klystron

2.3 Multi-cavity Klystrons

For the bandwidth of a two-cavity klystron to be sufficient for a television signal, the Q-values of its cavities would be low and its gain would be low. Furthermore, the overall amplitude/frequency characteristic would be unsuitable. It would be better from the point of view of selectivity and gain to cascade several stagger-tuned klystrons but the overall efficiency would then be extremely low. Instead, these several klystrons may all be combined into one; several stagger-tuned cavities may be cascaded along a common drift tube and coupled by one common beam as shown diagrammatically in Fig. 5. For television signals, four-cavity klystrons are used at the present time; typically, the input and output cavities have fairly low Q (about 80 to 100) and are both tuned to the centre frequency, the two intermediate cavities have higher Q (about 200 to 300) and are stagger-tuned to frequencies on either side of the centre frequency. In this way, an overall gain of about 36 dB, uniform within $\pm 0 \cdot 5$ dB over a bandwidth of up to 8 MHz, is readily obtained.
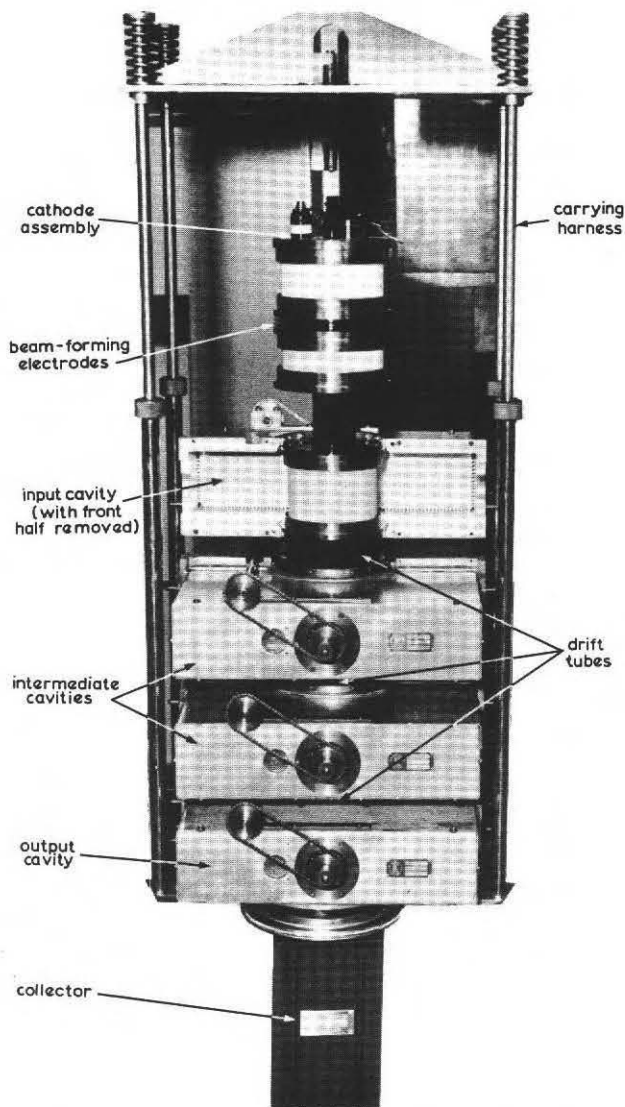
The theory of multi-cavity klystrons is extremely complex. Several writers have given theories of three-cavity klystrons but although they all involve approximations they nevertheless lead to acute computational difficulties. Curtice[9] uses the ballistic theory, Beck[6] uses a plasma theory, whilst Webber[10] uses a plasma theory for the region between the first and second cavity, and the ballistic theory for the region between the second and third cavity. The theories are very involved both because they include so many factors (e.g. the amplitude/frequency characteristic of each cavity and its coupling to the beam, and the length of each intermediate drift tube) and because the bunching of the beam is determined by the amplitude and phase of the voltage across each cavity that it has passed through. The problem has been surveyed by Curnow[11] who concludes that '. . . r.f. measurements under the actual operating conditions would appear to be essential if the best performance is to be obtained'.

It therefore appears impracticable to calculate the performance of four-cavity klystrons but, as suggested by O'Loughlin,[12] it is reasonable to suppose that the non-linearity in a multi-cavity klystron occurs principally in the drift space between the penultimate and output cavities. Up to a certain output power level, therefore, a four-cavity klystron may be represented by a two-cavity model the input cavity of which comprises a linear amplifier having the gain and frequency characteristics of the first three cavities. The experimental results described in the next section will be compared in Section 4 with theoretical results using the ballistic theory applied to this type of two-cavity model.

Fig. 6 — A four-cavity klystron (type K381) with one half of the input cavity removed

3. Experimental Results

3.1 General

Experiments were performed using a power amplifier, designed and made by The M.E.L. Equipment Co. Ltd, comprising an English Electric four-cavity klystron type K381 together with its power supplies and associated protective circuits. The klystron, shown in Fig. 6, comprised a cathode and beam-forming assembly, followed by four cascaded cavities and an air-cooled collector. The drift tubes and gaps were integral with the cathode and collector assemblies; the cavities were made in two halves which could be separately attached. The cavities were all of similar design, taking the form shown diagrammatically in Fig. 7. The whole was mounted vertically within a set of coils which, fed with direct current, produced the axial magnetic field necessary to focus the electron beam inside the drift tube assembly. A circulator forming part of the equipment was connected between the input to the amplifier and the input cavity of the klystron. The amplifier was

designed for use as a 'common amplifier' (i.e. to handle a combined sound and vision signal) and, for normal operation, the e.h.t. voltage (V_0 in Figs. 1 and 5) was 9 kV, the current through the focus coils was 9·1A; except where otherwise specified, these values were adopted for all results quoted in this monograph. With these values, the cathode current was 1·77A, the body current 10 mA to 20 mA (depending upon signal level) and the voltage across the focus coil 56V. Except for the small voltage drop across metering resistances, the collector was at earth potential. The heater supply was 13·1A at 13V. The rated saturated power of the klystron was 5 kW.

3.2 Gain/Frequency Characteristic

The nominal gain of the klystron was 36 dB; tuneable cavities were available which could be adjusted to achieve an amplitude/frequency characteristic uniform to within $\pm 0\cdot5$ dB over any 8 MHz bandwidth in the frequency range 590 MHz to 720 MHz. The damping on each cavity could be adjusted by rotating its coupling loop (see Fig. 7).

Fig. 8 — *Typical gain/frequency characteristic of the klystron under test*

Fig. 7 — *Cut-away view showing a drift-tube gap, resonator and coupling loop on K381 klystron*

The coupling loops in the intermediate cavities were connected to 50-ohm loads; damping on the input and output cavities was provided by the source and load impedances respectively.

Using a sweep signal generator, the input and output cavities were both tuned to the chosen centre frequency; the second and third cavities were stagger-tuned 4 MHz low and 4 MHz high respectively. Final adjustments were made to the tuning and the damping of all cavities so as to achieve an equi-ripple triple-humped response. For all experiments, the klystron was tuned to cover an 8 MHz bandwidth at or about Channel 46 (670 to 678 MHz).

The amplitude/frequency characteristic was found to depend, to a certain extent, upon the signal level. Fig. 8 shows a gain/frequency characteristic measured at low power levels during the early part of the tests. Its shape, whilst still uniform within $\pm 0\cdot5$ dB over the 8 MHz bandwidth, is significantly different from the equi-ripple

Fig. 9 — *Input/output characteristic*

--o--o-- ⎫
--x--x-- ⎬ Measured results
--●--●-- ⎭

———————— Theoretical result (see Section 4.2)

10

triple-humped response that was displayed by the sweep generator when the klystron was being tuned at high power. This effect will be discussed further in the next section.

3.3 Input/Output Characteristics

The measured variations of output power from the two intermediate cavities and the final cavity at the fundamental frequency, as a function of input power, are shown in Fig. 9. It is evident that the non-linearity occurs principally in the region between the third and final cavities, thus justifying the use of a two-cavity model to represent a four-cavity klystron. It also follows that the overall amplitude/frequency characteristic of the klystron will vary with output power in such a way that the characteristic of the output cavity will tend to dominate at high power levels. Thus, if the cavities are loaded and tuned so as to achieve a triple-humped overall response at high power levels, the central hump will be less pronounced at low power levels.

3.4 Levels of Harmonics

Levels of harmonics were measured using the arrangement shown block-schematically in Fig. 10. The level of an unmodulated signal from the signal generator was adjusted to achieve a given output power from the klystron. With the high-pass filter shown in Fig. 10 removed, and the variable attenuator set to 30 dB, a relative datum level of the signal at the fundamental frequency was measured on the receiver. With the high-pass filter inserted as shown in Fig. 10 and the variable attenuator set to zero insertion loss, the levels of the signals at the second and third harmonic frequencies were measured on the receiver, relative to the datum at the fundamental frequency. It was verified that negligible harmonic generation occurred in the receiver at the signal levels involved.

Similar measurements were made in which the output power of the klystron was measured as above but the remaining measuring system was connected by directional couplers to the damping loads on the two intermediate cavities. In this way, the levels of second and third harmonic in each intermediate cavity could be measured relative to the level of the fundamental component in that cavity, for given output power levels from the final cavity.

The results are shown in Fig. 11.

3.5 Levels of Intermodulation Products
3.5.1 Two-tone Tests

Levels of intermodulation products were measured using the arrangement shown block-schematically in Fig. 12. Two signals, at frequencies f_1 and f_2 (spaced 2 MHz apart and both within the pass-band of the klystron), were combined in a manner which minimized cross-modulation between them. The level of the input signal at f_1 was maintained at $+7$ dB relative to the level of that at f_2; the level of the combined signal was adjusted by the variable attenuator. The combined signal was amplified by a travelling-wave tube amplifier and applied to the klystron amplifier. It was verified that, at the low power levels involved (i.e. less than 10 W), negligible intermodulation occurred in the travelling-wave tube. A portion of the output power from the klystron was fed to a power meter and a narrow-band sweep receiver. The power levels of each of the two signals at f_1 and f_2 were determined in the absence of the other. The receiver was arranged to sweep sinusoidally, fifty times per second, over the bandwidth of the klystron and so to give a spectral display on the oscilloscope of all signals present in that bandwidth,
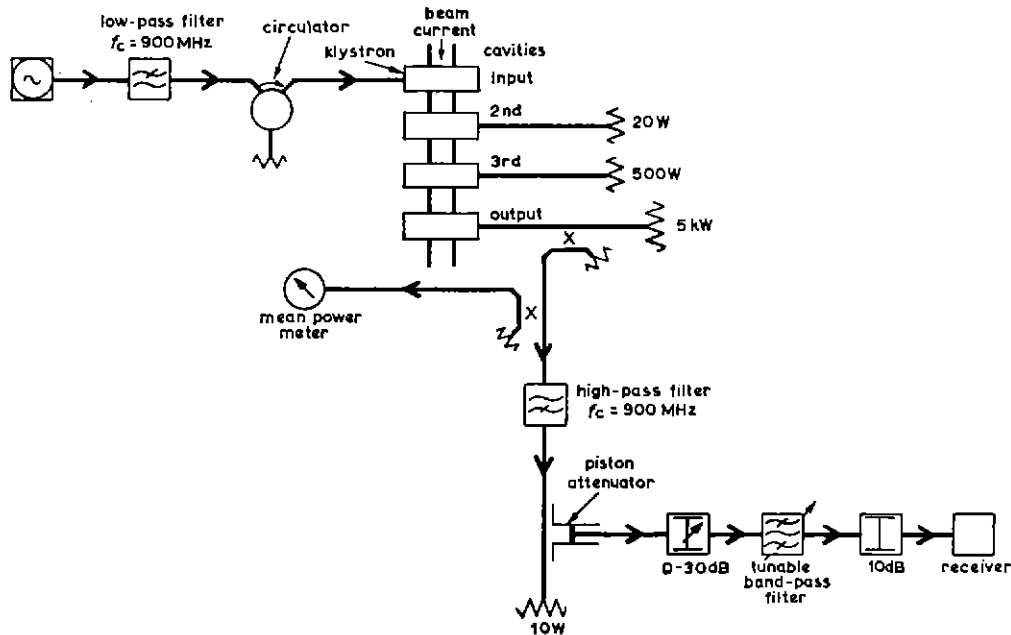
Fig. 10 — Arrangement used to measure levels of harmonic products

11

from which the level of each could be determined. The range of signal levels applied to the receiver was kept low enough to prevent intermodulation within the receiver. The levels of signals occurring at frequencies f_1, f_2, $(2f_1 - f_2)$ and $(2f_2 - f_1)$ were measured; the results are shown in Fig. 13.

3.5.2 Three-tone Tests

At translator stations the klystron amplifies the complete television signal comprising the modulated luminance, chrominance and sound signals. Under these conditions, the three carriers (i.e. the luminance, chrominance and sound carriers at frequencies f_v, f_c and f_s respectively) are all present simultaneously at comparatively high power under most picture conditions; their intermodulation product at frequency $(f_v + f_s - f_c)$ is dominant and, furthermore, it causes a bar pattern which is readily perceived subjectively. Subjective tests have shown that, for this pattern to be imperceptible, its level must not exceed -48 dB relative to peak sync. power. This requirement is so stringent that it forms the basis of one of the most important acceptance tests performed on klystrons for use at BBC translator stations. For test purposes, it is convenient to measure the level of this intermodulation term objectively under simulated picture conditions in which three c.w. input signals represent the three carrier components. Experience has shown that if the output levels of these signals at the frequencies of the luminance, chrominance and sound carriers are -8 dB, -17 dB and -7 dB relative to peak sync. power respectively, and the level of the $(f_v + f_s - f_c)$ intermodulation product is not greater than -52 dB relative to peak sync. power, then the pattern will be imperceptible subjectively under the great majority of

(b)

(a)
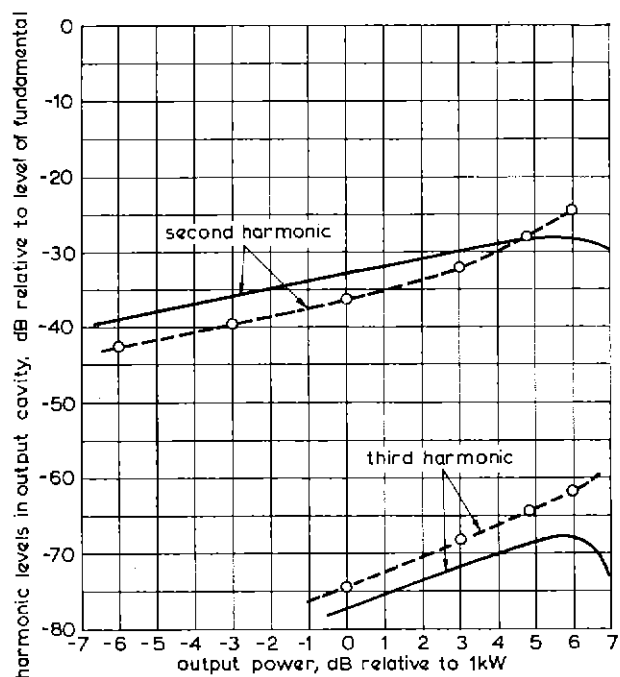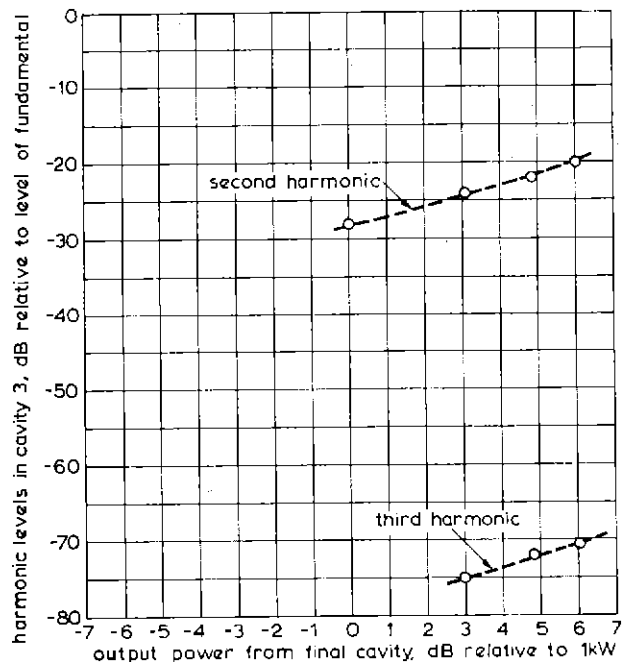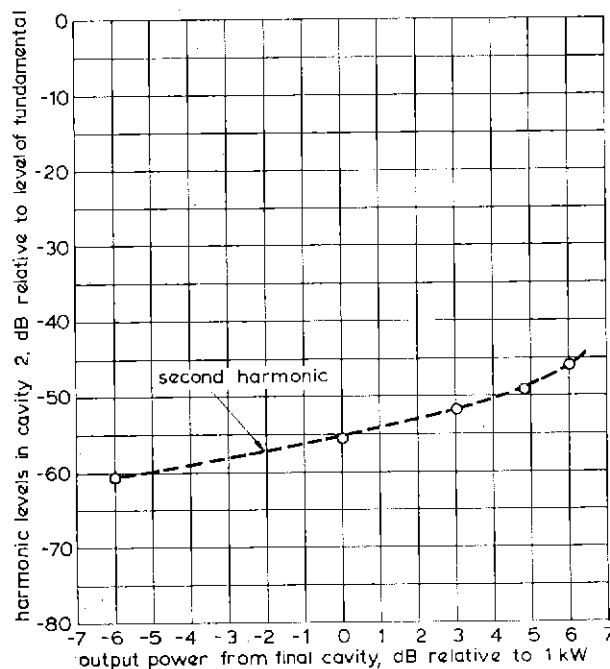
Note: Levels of 3rd Harmonic were immeasurably small, i.e. less than -80 dB

(c)

Fig. 11 — Levels of harmonics

(a) in output cavity
(b) in cavity 3
(c) in cavity 2

--o--o--   Measured results
—————   Theoretical results (see Section 4.3)

12
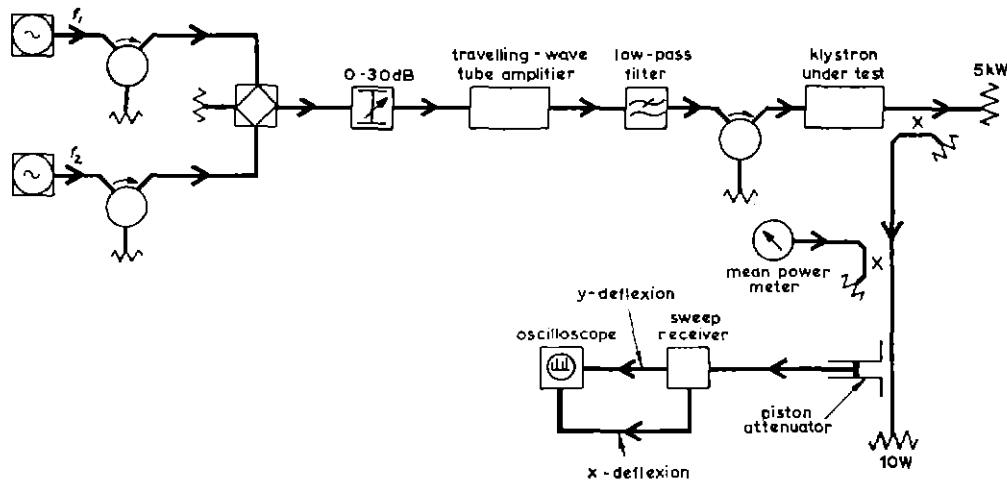
Fig. 12 — *Arrangement used to measure levels of intermodulation products*

picture conditions. Those levels have therefore been adopted as standard and the test has become known as the 'three-tone test'. This intermodulation product is usually the dominant feature when klystrons are used at translator stations and, to achieve the specified level of − 52 dB, the peak sync. power fed to the aerial must not, at the present time, exceed one-fifth of the klystron saturated power. As will be shown, the theoretical level from an ideal klystron is about − 55 dB when de-rated in that way and, in practice, levels from − 47 dB to − 52 dB are typical,[12] depending upon the tuning and the loading of the cavities.

This test was carried out, as part of the general investigation described in this monograph, using an arrangement similar to that shown in Fig. 12. When delivering a peak

Fig. 13 — *Levels of two-tone intermodulation products*

--o--o-- ⎫
--x--x-- ⎬ Measured results
--●--●-- ⎪
--Δ--Δ-- ⎭
——————— Theoretical results (see Section 4.4.1)

sync. power of 1 kW, the measured level of the intermodulation product at $(f_v + f_s - f_c)$ was − 47 dB relative to 1 kW. This level would be unacceptable for service use but, in practice, an acceptable level would be achieved by adjusting the tuning and loading of the cavities, as discussed in Section 4.4.2.

3.6 Differential Amplitude Characteristics

The results given in Fig. 13 show that the weaker of two signals (at f_2 in Fig. 13) is 'crushed' by the stronger signal. A similar situation arises in the case of a colour signal in that the amplitude of the chrominance signal is reduced by the presence of the (stronger) luminance signal. The result is termed 'differential amplitude distortion' or 'differential gain distortion'; its effect is to reduce the saturation of a colour picture when its brightness decreases.*

The differential amplitude distortion caused by the klystron was measured using the equipment shown block-schematically in Fig. 14. The video signal shown in Fig. 15 (comprising a seven-step luminance signal with a colour sub-carrier of constant amplitude at 4.43 MHz on each step) was modulated on a Channel 33 carrier, frequency-changed to Channel 46, and applied to the klystron. A receiver having 2 MHz i.f. bandwidth was tuned to the chrominance signal at the output of the klystron; the un-detected i.f. output was displayed on an oscilloscope (Fig. 16). This display, which is equivalent to the envelope of the chrominance signal when the luminance signal has been removed, enabled the distortion caused by the klystron to be assessed without introducing additional distortions attributable to detection.

The resulting waveforms, corresponding to peak sync. powers of 1 kW and 3 kW, are given in Fig. 16. They show the positions of the sync. pulses (during which the chrominance signal is zero) followed by the colour bursts, followed by the waveform of the chrominance signal that

---

* Because negative modulation is used, the transmitted luminance signal increases as the brightness decreases.

13
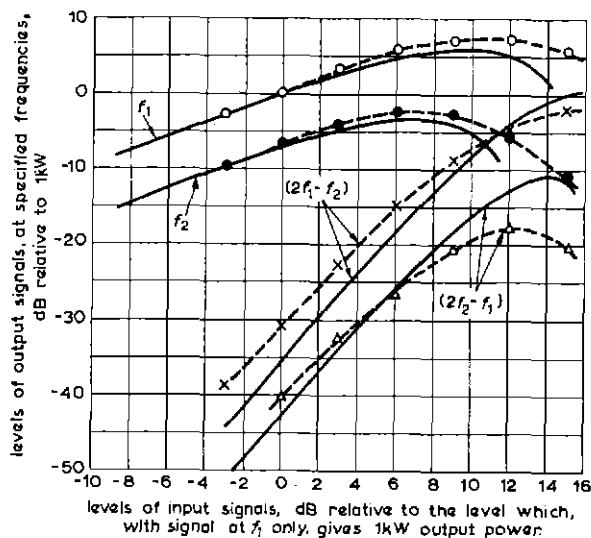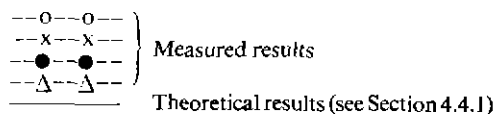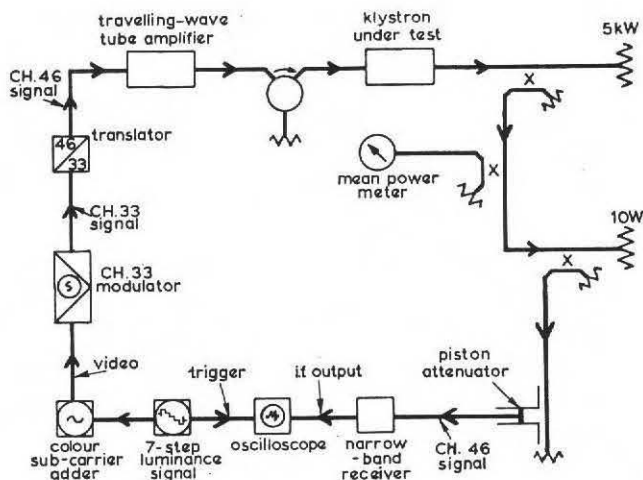
Fig. 14 — Equipment used to measure differential amplitude distortion

(a)

occurs during each of the eight levels of luminance of the test waveform shown in Fig. 15. When the klystron was delivering only 1 kW peak sync. power (Fig. 16(a)) it was operating in a near-linear condition and the amplitude of the chrominance signal remained nearly constant over all the eight levels of the luminance signal. When delivering 3 kW peak sync. power (Fig. 16(b)), however, the non-linearity of the klystron was evidenced by the crushing of the chrominance signal at relatively high luminance-carrier levels. Thus, for example, when the luminance component of the test waveform (Fig. 15) corresponded

(b)

Fig. 16 — Waveforms of chrominance signals showing differential amplitude distortion
(a) 1 kW peak sync. power   (b) 3 kW peak sync. power
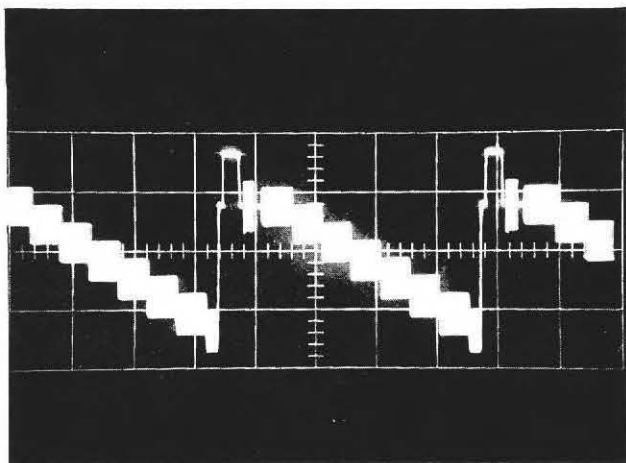
Fig. 15 — Video waveform of test signal used to measure differential amplitude and differential phase distortions

to black level (77 per cent modulation depth) immediately following the colour burst, the amplitude of the chrominance signal at the output of the klystron (Fig. 16) was reduced below its correct value. As the amplitude of the luminance carrier progressively decreased to the value corresponding to peak white (19 per cent modulation depth), the amplitude of the chrominance signal recovered to its correct value. The effect which this has on a colour

picture is to change the saturation of a coloured object if its brightness varies. This is termed differential amplitude distortion and is expressed in terms of the percentage change of amplitude of the chrominance signal when the luminance signal varies from black level to peak white (see Section 4.5). The waveforms shown in Fig. 16 indicate that, when delivering 1 kW, the klystron causes 4 per cent differential amplitude distortion; when delivering 3 kW the distortion increases to 22 per cent.

It was not possible to carry out this test in the presence of a sound signal because the latter could not be separated sufficiently well from the colour signal for display purposes. A separate experiment, however, displaying the detected output from a vestigial-sideband (v.s.b.) receiver showed that, at 1 kW peak sync. power output, the presence of the sound carrier made only very slight difference to the distortion. The 1 kW condition above therefore corresponds to typical operation at translator stations:

14

the 3 kW condition approximates to operational conditions where separate sound and vision amplifiers are used.

3.7 *Differential Phase Characteristics*

When the klystron is not driven, the beam power (i.e. the product of the beam current and the beam voltage) is dissipated at the collector. When the klystron is driven, the beam power is unchanged but some of it is converted to r.f. power and, consequently, the power dissipated at the collector is reduced. Since the mean beam current is unaffected, this means that the mean velocity of the electrons is reduced as the klystron is driven harder. Thus the group delay of the klystron increases as its output power is increased. The result is termed 'differential phase distortion' or 'level-dependent phase distortion';* its effect is to alter the hue of a colour signal when its brightness varies. This is not a very marked effect with klystrons, however, because the reduction of mean electron velocity occurs mainly towards the far end of the drift tube and the overall change of group delay is small. On the other hand, a few degrees of differential phase distortion is readily perceptible subjectively and, at stations where the peak sync. power approaches the saturated power rating of the klystron, it may be necessary to pre-correct the phase of the colour sub-carrier in order to allow for subsequent differential phase distortion in the klystron. The current BBC specification requires that the resulting differential phase distortion does not exceed $\pm 3°$, whilst that without pre-correction does not exceed $\pm 10°$.

Two methods were adopted to measure the differential phase characteristics of the klystron. The first method used the standard 'staircase' luminance signal, with superimposed colour sub-carrier. For this, apparatus similar to that shown block-schematically in Fig. 14 was employed, but with the narrow-band receiver replaced by a v.s.b. receiver of the type normally used for re-broadcast reception. The output from its detector was fed through a 4·43 MHz band-pass filter to a colour signal analyser the output of which was displayed on the oscilloscope. The amplitude of the output signal from the colour signal analyser was proportional to the phase of the input signal relative to that of a reference signal obtained from the colour sub-carrier adder. The changes of phase of the colour signal caused by changes of amplitude of the associated luminance signal could therefore be measured. These phase changes were found to be very small; they were not only so small as to make their measurement very difficult against the background noise through the complete chain but, more significantly, the differential phase distortion measured when the klystron was included in the measuring chain was comparable with that caused by the chain itself. As far as could be judged, the differential phase distortion introduced by the complete chain, including the klystron, was about 3° for peak sync. output powers up to 3 kW, whilst that introduced by the chain, with the klystron by-

passed, was about 2°. Clearly, the distortion caused by the klystron itself cannot be deduced from these results. For this reason, a second method[13] for measuring the change of phase was adopted, using the equipment shown block-schematically in Fig. 17. The output from a signal genera-
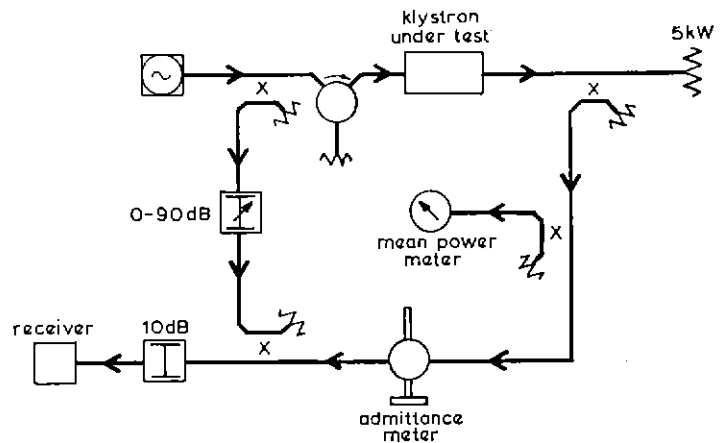
Fig. 17 — Arrangement used to measure level-dependent phase shift

tor was fed to a receiver through two parallel paths, one of which was a reference path and the other of which included both the klystron under test and an admittance meter. By adjusting the controls on the admittance meter to maintain zero output from the receiver, changes of amplitude and phase of the signal through the klystron could be deduced from the meter readings. The results are shown as a function of frequency in Fig. 18 for changes of
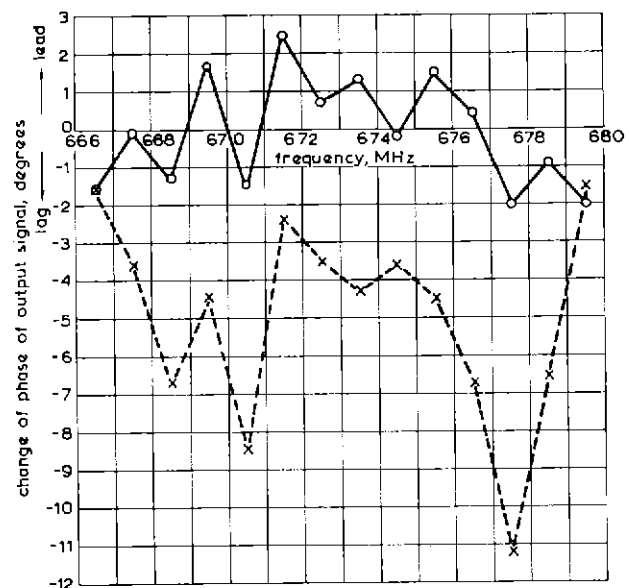
Fig. 18 — Change of phase of output signal caused by change of output power

—o——o— Change of output power 100 watts to 1 kW
--x--x--- Change of output power 100 watts to 3 kW

---

* This effect is also sometimes termed 'amplitude-to-phase conversion', particularly in connexion with systems using frequency modulation.

15

output power from 100 watts to 1 kW and from 100 watts to 3 kW. The results exhibit a scatter because the inherent accuracy of the method is about $\pm 3°$.[13] For output powers up to 1 kW, the klystron imposes a phase change whose mean value taken over the channel bandwidth is $0 \cdot 1°$. This value increases to 5° when the output power is about 3 kW. It is difficult to relate this result to the occurrence of differential phase distortion of a television signal, however, because the latter corresponds to the change of phase of a small r.f. signal of constant amplitude (the colour sub-carrier) caused by changes of amplitude of another r.f. signal (the luminance carrier). If necessary, the method could be applied to that case, using two input signals, but it would be complicated and the overall accuracy would probably be no better than that of the former method. In any case, both methods of measurement imply that the phase change introduced by the klystron is well within the specified limit of $\pm 10°$.

3.8 *Change of Phase of Output Signal With Beam Voltage*

The equipment shown block-schematically in Fig. 17 was used to measure changes of phase of the output signal from the klystron as a function of changes made to the beam voltage. The results, measured at 675 MHz, are shown in Fig. 19.
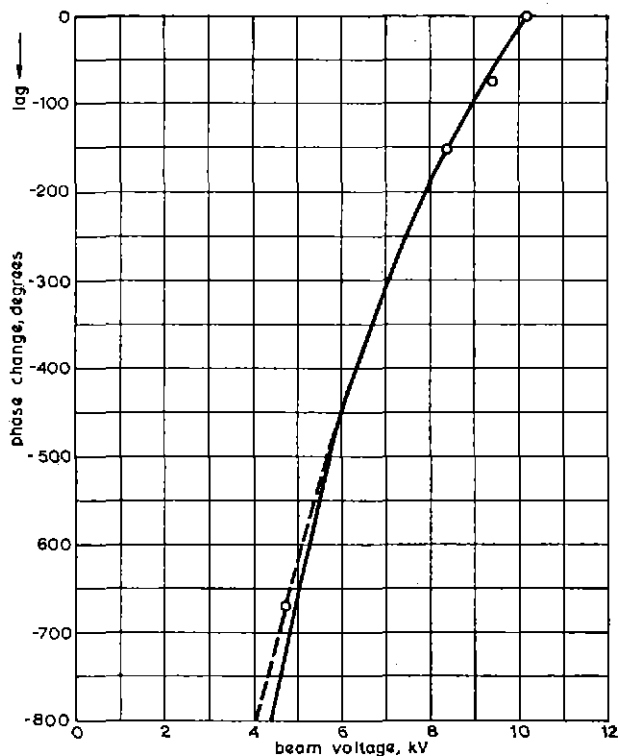
Fig. 19 — Change of phase of output signal with beam voltage

--o--o-- Measured result
———— Theoretical result (see Section 4.7)

4. Comparison of Theoretical and Measured Results

4.1 *General*

The following theoretical results are calculated using the ballistic theory discussed in Sections 2.2 and 2.3. The effect of de-bunching is neglected; as discussed in Section 2.2.1, this is valid for small signals but it may not be valid as the saturated power level is approached. It is further assumed, as discussed in Section 2.3, that the non-linear behaviour occurs entirely in the drift space between the penultimate and output cavities. The four-cavity klystron used for the tests is therefore regarded, for calculation purposes, as a two-cavity klystron preceded by a linear amplifier. This also is valid for small signals but it may lead to error as the saturated power level is approached.

Suppose the input signal voltage at frequency f_r is a fraction, k_r, of that voltage which, in the absence of other input signals, gives saturated output power P_0. Then, since the first maximum of $J_1(x)$ is equal to $0 \cdot 582$ and occurs when $x = 1 \cdot 84$, $K_r = 1 \cdot 84 k_r$, and Equations (5) and (6) may be re-written as

$$\left(\frac{P_{mnp}}{P_0}\right)^{\frac{1}{2}} = \frac{F_{mnp}}{0 \cdot 582} \cdot J_m(a) \cdot J_n(\beta) \cdot J_p(\gamma) \qquad (7)$$

where P_{mnp} is the power output at frequency $(mf_1 + nf_2 + pf_3)$

$$a = 1 \cdot 84 k_1 (mf_1 + nf_2 + pf_3)/f_1$$
$$\beta = 1 \cdot 84 k_2 (mf_1 + nf_2 + pf_3)/f_2 \qquad (8)$$
$$\gamma = 1 \cdot 84 k_3 (mf_1 + nf_2 + pf_3)/f_3$$

and F_{mnp} is a factor depending upon the amplitude/frequency characteristics of the klystron cavities.

The factor k_r will be termed the 'normalized bunching parameter'.

Unless otherwise stated, all the calculations in this section assume P_0 to be 5 kW, the rated saturated power of the klystron used for the experiments.

4.2 *Input/Output Characteristic*

When only one input signal is applied, $k_2 = k_3 = 0$ in Equation (8). Similarly, since only the output at the fundamental frequency is being considered, $m = 1$, and $n = p = 0$. The theoretical input/output characteristic is therefore given by

$$\left(\frac{P_{100}}{P_0}\right)^{\frac{1}{2}} = \frac{1}{0 \cdot 582} J_1(1 \cdot 84 k_1) \qquad (9)$$

This is drawn in Fig. 9 for comparison with the measured input/output characteristic.

4.3 *Levels of Harmonics*

To calculate the harmonic levels, $k_2 = k_3 = n = p = 0$ as in Section 4.2. The level of the mth harmonic is therefore given by

$$\left(\frac{P_{moo}}{P_0}\right)^{\frac{1}{2}} = \frac{F_{moo}}{0.582} J_{moo}(1.84mk_1) \qquad (10)$$

The factor F_{moo} represents the response of the output cavity at the frequency of the mth harmonic relative to that at the fundamental frequency. It is a very difficult factor to measure because it includes the coupling between the beam and the cavity; it is also a difficult factor to calculate both because of the geometrical shape of the cavity and because the cavity is loaded at its centre by the admittance

both of the beam and of the gap and ceramic tube (see Fig. 7). The factor was therefore assessed partly by calculation and partly by measurement as follows.

A small test probe was inserted in the cavity in addition to, and near the face remote from, the existing output coupling loop. The amplitude/frequency characteristic of the cavity, from the test probe to the coupling loop was measured over three frequency bands in the region of the fundamental, second and third harmonic frequencies of operation of the klystron. The results are shown in Fig. 20. These results apply over the small bands of frequency shown but they cannot be related to each other because the variation of coupling of the test probe to the cavity is not known over the whole frequency range. It is clear from Fig. 20(b) that a resonant mode exists in the cavity at approximately twice the frequency of the fundamental mode, and that it is a mode which couples to the beam.

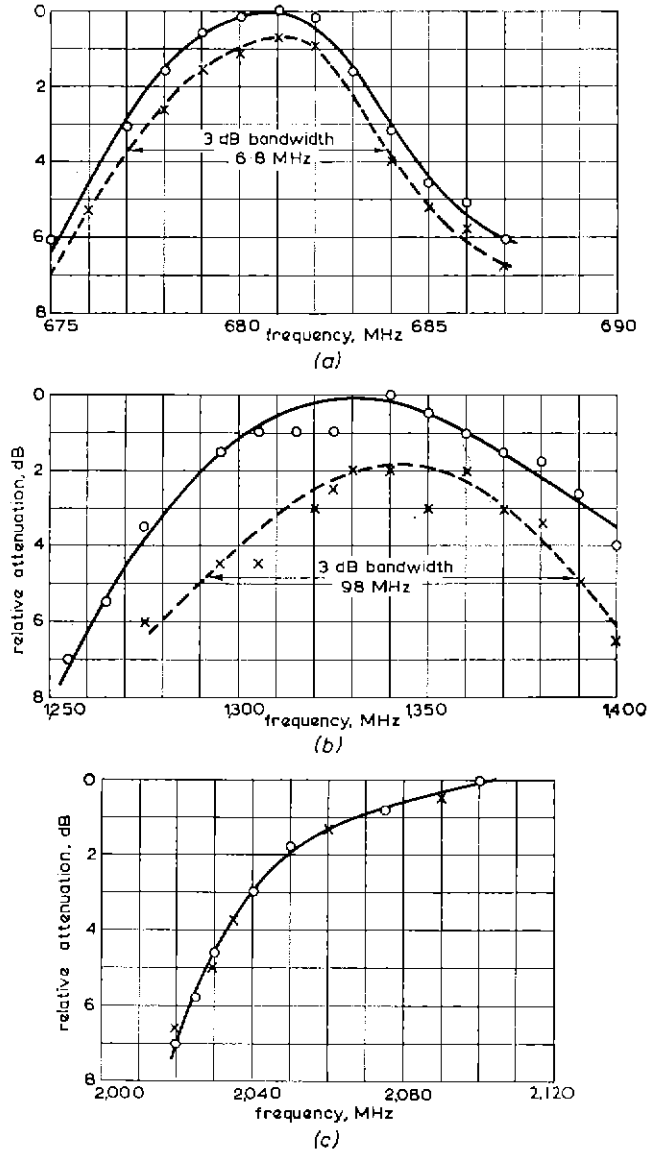Assuming each cavity to operate in the TE_{011} mode, the

Fig. 20 — Amplitude/frequency characteristics of output cavity

(a) At fundamental frequencies
(b) At second-harmonic frequencies
(c) At third-harmonic frequencies

—o——o— With beam off
—x——x— With beam on
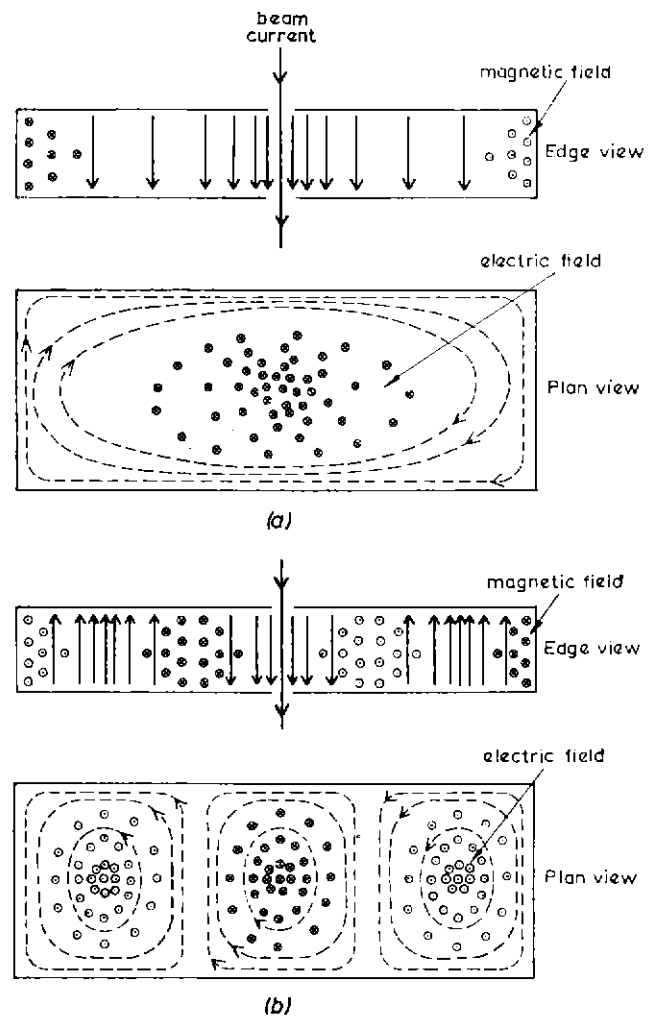
Fig. 21 — Field patterns in the output cavity

(a) Fundamental mode   (b) Third-order mode

———————— Electric field
— — — — — Magnetic field

17

field patterns for the fundamental and third-order resonant conditions will be as shown in Figs. 21(a) and 21(b). It may appear at first sight that the third-order resonance should occur at three times the fundamental resonant frequency but this is not so for two reasons. First, the wavelength in the cavity is not inversely proportional to frequency, particularly when, as is the case for the cavity in question, the fundamental resonant mode occurs at very nearly the cut-off frequency. Second, the effect of the admittance corresponding to the loading of the beam, the ceramic tube, and the beam coupling gap, across the centre of the cavity, is such as further to affect this relationship. The approximate analysis given in the Appendix (Section 10.2) shows that the amplitude/frequency characteristic of the cavity would take the form of the dotted curve shown in Fig. 22 if the cavity were loss-less. It is evident that the third-order resonance occurs at very nearly twice the frequency of the fundamental resonance. The effect of loss in the cavity (notably, of course, the effect of the load impedance coupled into the cavity) can be assessed in conjunction with Fig. 20. Thus, the peak at 681 MHz on the curve of Fig. 22 can be 'rounded-off' to have a 3 dB bandwidth of 6·8 MHz corresponding to that in Fig. 20(a); the peak at 1,340 MHz can be rounded-off to have a 3 dB

bandwidth of 98 MHz corresponding to that of Fig. 20(b). The curve of Fig. 20(c) is in general agreement with that of Fig. 22 over the range 2,000 to 2,100 MHz.

The overall amplitude/frequency characteristic of the cavity is therefore taken to be as shown in Fig. 22; relative to the fundamental, the cavity attenuates the second harmonic by 27 dB, the third harmonic by 62 dB. Evaluating Equation (10) with these values of F_{moo} gives the theoretical results shown in Fig. 11(a). Agreement between the measured and theoretical results is well within the accuracy to which the factor F_{moo} is known.

It should be noted that the above is only an approximate assessment of the theoretical harmonic levels; apart from the approximations in the theory of the klystron, no allowance has been made, for example, for possible variations with frequency of the coupling from the cavity to the load. Nevertheless, there is no doubt that cavities of this design exhibit a third-order resonance at about the second harmonic frequency when the cavity is tuned to about 680 MHz; Fig. 23, for example, shows the measured overall gain/frequency characteristic of the klystron at about 1,354 MHz when the cavities were tuned to give the response shown in Fig. 8. Surprisingly, the klystron had 20 dB overall gain at 1,354 MHz. This effect, however, is
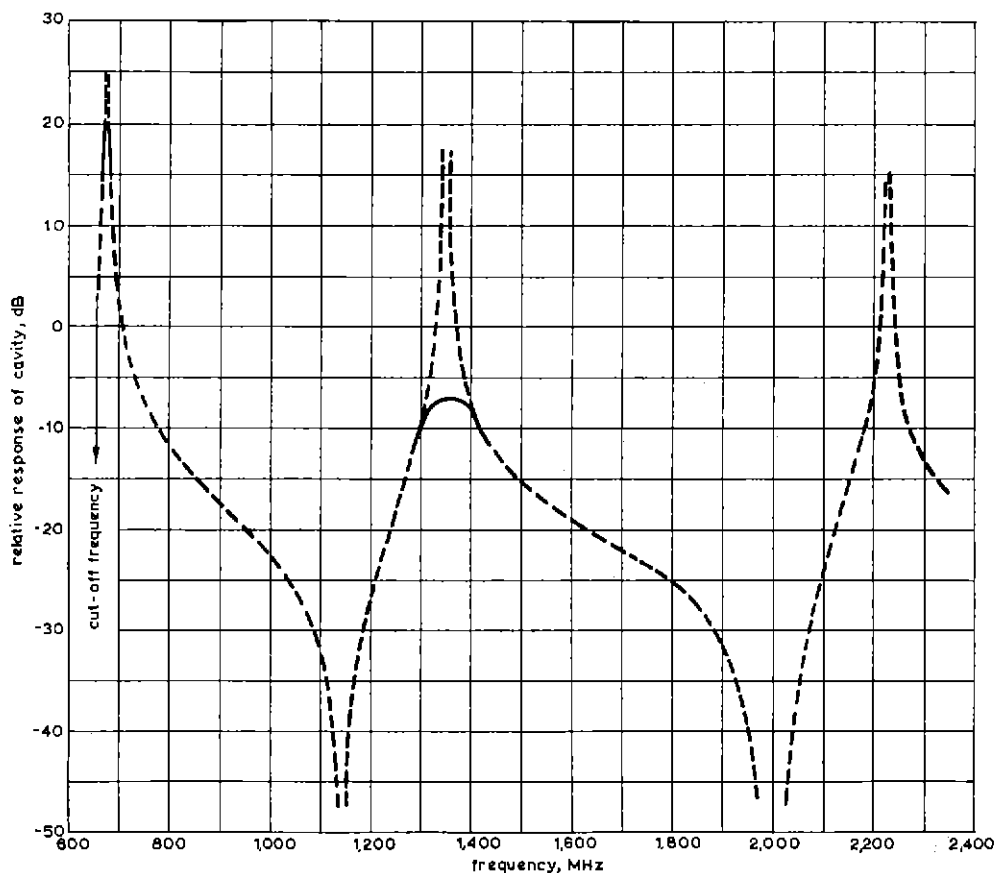
Fig. 22 — Estimated amplitude/frequency characteristic of output cavity

– – – – Theoretical response neglecting loss ———— Allowance for loss

18
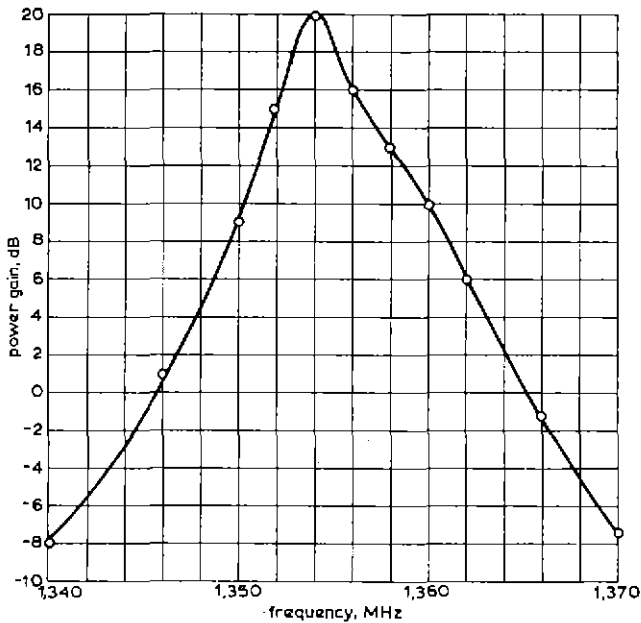
Fig. 23 — Overall gain of klystron in the neighbourhood of the second-harmonic frequency

likely to occur only when the cavity is tuned to a particular fundamental frequency and is not general at all tuned frequencies. Furthermore, harmonic filters following the klystron would provide adequate harmonic suppression at the great majority of transmitting stations. Nevertheless, the effect should be borne in mind and, if the required harmonic suppression is particularly stringent at a few stations, it would be desirable to insert shorting posts across the output cavity so as to inhibit the third-order resonance and so to gain harmonic suppression within the klystron itself.

4.4 Levels of Intermodulation Products

4.4.1 Two-tone Tests

When only two input signals are applied, $k_3 = 0$ in Equation (8).

If the output signal at $(2f_1 - f_2)$ is being considered, $m = 2$, $n = -1$, and $p = 0$. If the frequencies f_1 and f_2 are nearly equal, then

$$a = 1 \cdot 84 k_1 (2f_1 - f_2)/f_1 \approx 1 \cdot 84 k_1$$

and

$$\beta = 1 \cdot 84 k_2 (2f_1 - f_2)/f_2 \approx 1 \cdot 84 k_2$$

Equation (7) may therefore be re-written:

$$\left(\frac{P_{210}}{P_0}\right)^{\frac{1}{2}} = \frac{F_{210}}{0 \cdot 582} \cdot J_2(1 \cdot 84 k_1) \cdot J_1(1 \cdot 84 k_2) \qquad (11)$$

where P_{210} represents the output power at frequency $(2f_1 - f_2)$.

Likewise, if the output at f_2 is being considered, $m = 0$, $n = 1$, $p = 0$ in Equation (8) and

$$\left(\frac{P_{010}}{P_0}\right)^{\frac{1}{2}} = \frac{F_{010}}{0 \cdot 582} \cdot J_0(1 \cdot 84 k_1) \cdot J_1(1 \cdot 84 k_2) \qquad (12)$$

where P_{010} represents the output power at frequency f_2. It is apparent that the term $J_0(1 \cdot 84 k_1)$ accounts for the 'crushing' of a weak signal by a strong one that is observed in practice.

The factors F_{210} and F_{010} in Equations (11) and (12) represent the amplitude/frequency characteristics of the klystron cavities. Whilst the overall amplitude/frequency characteristic of the klystron can be taken as constant over the frequency band being considered (see Fig. 8), this is the overall result of four stagger-tuned responses which, individually, are not uniform. The amplitude/frequency characteristic of the final cavity is as sketched in Fig. 24;
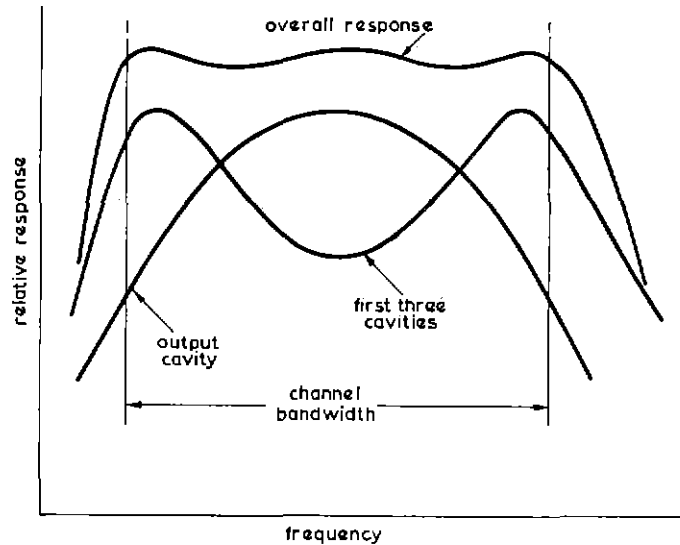
Fig. 24 — Typical amplitude/frequency characteristics of a four-cavity klystron

the overall response of the first three cavities must therefore be the complement, as also sketched in Fig. 24. As O'Loughlin has pointed out,[12] the levels of signals applied at the input to the klystron are modified by this complementary response before leaving the third cavity and, strictly, the values of k_1 and k_2 should be modified accordingly. Furthermore, the level of the signal being considered should be modified according to the amplitude/frequency characteristic of the output cavity. The factors F_{210} and F_{010} imply this complete modification but, in practice, this changes the levels of the signals by only a few decibels and, bearing in mind the other approximations involved, this modification has been ignored. Taking these factors as unity throughout, levels of the signals at f_1, f_2, $(2f_1 - f_2)$ and $(2f_2 - f_1)$ have been calculated using equations similar to (11) and (12); they are shown for comparison with measured results in Fig. 13. Agreement is good for output powers up to at least half the saturated

19

power, and thereafter the theoretical results give a good estimate of the levels that occur in practice.

4.4.2 Three-tone Tests

As discussed in Section 3.5.2, the 'three-tone test' is generally taken to mean a test carried out at translator stations to measure the amplitude of the intermodulation term at frequency $(f_v - f_c + f_s)$ when three signals of prescribed relative levels are applied simultaneously at frequencies f_v, f_c and f_s, the frequencies of the vision, colour and sound carriers respectively. In this case, $m = p = 1$ and $n = -1$ in Equation (8) and, since all the frequencies involved are nearly equal

$$\alpha = 1 \cdot 84 k_v (f_v - f_c + f_s)/f_v \approx 1 \cdot 84 k_v$$

$$\beta = 1 \cdot 84 k_c (f_v - f_c + f_s)/f_c \approx 1 \cdot 84 k_c$$

$$\gamma = 1 \cdot 84 k_s (f_v - f_c + f_s)/f_s \approx 1 \cdot 84 k_s$$

Thus

$$\left(\frac{P_{111}}{P_0}\right)^{\frac{1}{2}} = \frac{F_{111}}{0 \cdot 582} \cdot J_1(1 \cdot 84 k_v) \cdot J_1(1 \cdot 84 k_c) \cdot J_1(1 \cdot 84 k_s) \quad (13)$$

where P_{111} represents the output power at the frequency $(f_v - f_c + f_s)$ and F_{111} is an amplitude/frequency factor having a significance similar to that of the factors F_{210} and F_{010} discussed in the previous section.

It follows from Equation (9) that

$$J_1(1 \cdot 84 k_v) = 0 \cdot 582 \left(\frac{P_{100}}{P_p}\right)^{\frac{1}{2}} \cdot \left(\frac{P_p}{P_0}\right)^{\frac{1}{2}}$$

$$J_1(1 \cdot 84 k_c) = 0 \cdot 582 \left(\frac{P_{010}}{P_p}\right)^{\frac{1}{2}} \cdot \left(\frac{P_p}{P_0}\right)^{\frac{1}{2}} \quad (14)$$

and $\quad J_1(1 \cdot 84 k_s) = 0 \cdot 582 \left(\frac{P_{001}}{P_p}\right)^{\frac{1}{2}} \cdot \left(\frac{P_p}{P_0}\right)^{\frac{1}{2}}$

where P_{100}, P_{010} and P_{001} represent the output powers at f_v, f_c and f_s respectively, and P_p represents the peak sync. output power. Combining Equations (13) and (14) gives

$$\left(\frac{P_{111}}{P_0}\right)^{\frac{1}{2}} = (0 \cdot 582)^2 F_{111} \left(\frac{P_p}{P_0}\right)^{\frac{1}{2}} \cdot \left(\frac{P_{100}}{P_p}\right)^{\frac{1}{2}} \cdot \left(\frac{P_{010}}{P_p}\right)^{\frac{1}{2}} \cdot \left(\frac{P_{001}}{P_p}\right)^{\frac{1}{2}}$$

$$\therefore \left(\frac{P_{111}}{P_p}\right)^{\frac{1}{2}} = (0 \cdot 582)^2 F_{111} \cdot \frac{P_p}{P_0} \cdot \left(\frac{P_{100}}{P_p}\right)^{\frac{1}{2}} \cdot \left(\frac{P_{010}}{P_p}\right)^{\frac{1}{2}} \cdot \left(\frac{P_{001}}{P_p}\right)^{\frac{1}{2}} \quad (15)$$

If the output powers at f_v, f_c and f_s are $-v$ dB, $-c$ dB and $-s$ dB relative to peak sync. power respectively, peak sync. power is $-p$ dB relative to saturated power, and the factor F_{111} is taken to be unity, Equation (15) can be expressed in the convenient form

Level of intermodulation product at

$$(f_v - f_c + f_s) = -(9 \cdot 4 + 2p + v + c + s) \text{ dB}$$

relative to peak sync. power

For the three-tone test, the accepted values of v, c and s are 8 dB, 17 dB and 7 dB respectively. If the peak sync. power is -7 dB relative to the klystron saturated power, it follows that the level of the intermodulation product will be $-(9 \cdot 4 + 14 + 8 + 17 + 7) \text{dB} = -55 \cdot 4$ dB relative to peak sync. power. It also follows that the level of this product will vary 'decibel for decibel' as the level of either of the three signals is varied, or as '2 dB for every 1 dB' as the ratio of peak sync. power to saturated power is varied. Variations of this type are found to occur in practice.

Using a different analysis, O'Loughlin[12] gives a predicted level of $-55 \cdot 5$ dB for this intermodulation term, assuming the factor F_{111} to be unity. He shows theoretically that the effect of this factor (depending upon the tuning and loading of the cavities) can typically be such as to increase the level of the intermodulation term by up to $7 \cdot 5$ dB. This is found to be true in practice and, generally, the cavities are tuned so as to achieve not only a suitable gain/frequency characteristic but also an acceptable level for this particular intermodulation term.

4.5 Differential Amplitude Characteristics

Differential amplitude distortion on a television signal is specified in terms of the change of amplitude of a chrominance signal when superimposed on the eight levels of a seven-step luminance staircase between black and peak white as discussed in Section 3.6; this type of distortion is caused in a klystron by the 'crushing' effect that a strong signal has on a weak signal. This can be represented in Equation (8) by putting $f_1 = f_v$ and $k_1 = k_v$ corresponding to the luminance signal, $f_2 = f_c$ and $k_2 = k_c$ corresponding to the chrominance signal, and $k_3 = 0$. If the amplitude of the term at f_v is being considered, $m = 1$, $n = 0$, $p = 0$ and, since $f_v \approx f_c$, Equation (7) can be written as

$$\left(\frac{P_{100}}{P_0}\right)^{\frac{1}{2}} = \frac{1}{0 \cdot 582} \cdot J_1(1 \cdot 84 k_v) \cdot J_0(1 \cdot 84 k_c) \quad (16)$$

where P_{100} represents the output power of the luminance signal.

Correspondingly

$$\left(\frac{P_{010}}{P_0}\right)^{\frac{1}{2}} = \frac{1}{0 \cdot 582} \cdot J_0(1 \cdot 84 k_v) \cdot J_1(1 \cdot 84 k_c) \quad (17)$$

where P_{010} represents the output power of the chrominance signal.

The terms in $J_0(\ )$ in Equations (16) and (17) indicate the degree of crushing that occurs. Since k_c is small, $J_0(1 \cdot 84 k_c)$ is nearly unity, thus negligible crushing is caused on the luminance signal by the chrominance signal. As saturated power is approached, k_v approaches unity and $J_0(1 \cdot 84 k_v)$ becomes significantly less than unity, showing that crushing is caused on the chrominance signal by the luminance signal. The differential amplitude distortion is given by

$$D = \left[1 - \frac{J_0(1 \cdot 84 k_{v2})}{J_0(1 \cdot 84 k_{v1})}\right] 100 \text{ per cent} \quad (18)$$

20

where k_{v1} and k_{v2} are the normalized bunching parameters at the luminance carrier frequency. They give the two levels of luminance signal that define the range within which the distortion is being considered.

The maximum distortion will be that corresponding to a change of luminance signal from peak white to black level (i.e. as the luminance carrier amplitude increases from 19 per cent to 77 per cent of the peak sync. amplitude). It has been calculated from Equation (18) over this range of luminance amplitude; the results are shown in Fig. 25 as a
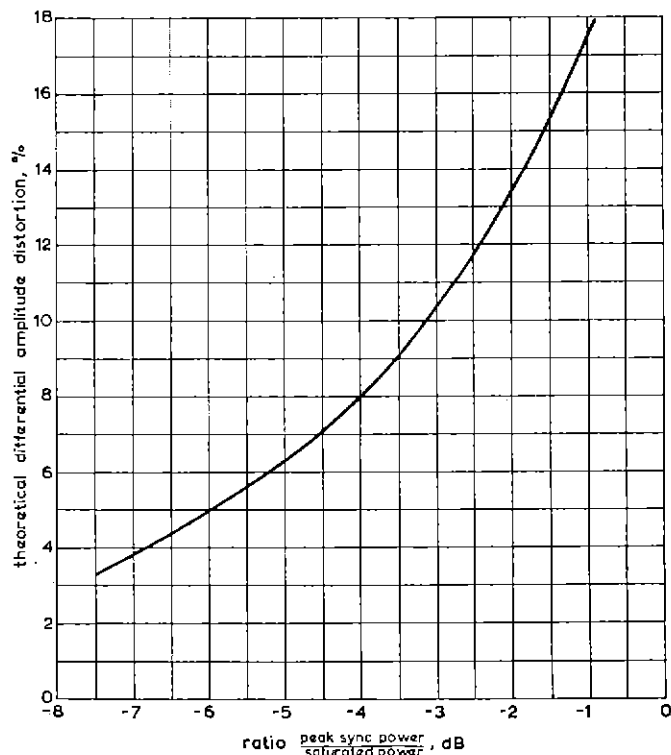
Fig. 25 — *Theoretical differential amplitude distortion*

function of peak sync. output power. These agree well with the measured result at 1 kW output power (see Section 3.6) but tend to be optimistic when compared with the measured result at 3 kW output power. This disparity may be associated with the variation of the gain/frequency characteristic with output power discussed in Section 3.3.

4.6 *Differential Phase Characteristics*

As discussed in Section 3.7, some of the d.c. beam power of the klystron is converted to r.f. power, and diverted to the intermediate cavities, when the klystron is driven. As a result, the group delay and, therefore, the differential phase of the chrominance signal increases with change of luminance signal level because the output power is a function of the level of this signal.

The mean power carried by the beam across any section

of the drift tube must be equal to the beam power ($I_0 V_0$) less any r.f. power which it has delivered at intermediate cavities. Thus

$$\frac{\overline{u_a^2} I_0}{2\eta} = V_0 I_0 - P_{rf} \qquad (19)$$

where $\overline{u_a^2}$ is the mean squared velocity of the electrons forming the beam at the chosen cross-section and P_{rf} represents the total r.f. power delivered at intermediate cavities. Since the spread of velocities about the mean value (Δ in Equation (2)) is small, the mean squared velocity can be taken to be equal to the mean velocity squared (i.e. terms in Δ^2 can be neglected in comparison with unity). The mean velocity of the beam at this section can therefore be written as

$$u_a = \left(\frac{2\eta}{I_0}[V_0 I_0 - P_{rf}]\right)^{\frac{1}{2}} \qquad (20)$$

Combining Equations (1) and (20) gives

$$\frac{u_a}{u_0} = \left(1 - \frac{P_{rf}}{V_0 I_0}\right)^{\frac{1}{2}} \qquad (21)$$

In a four-cavity klystron, there are therefore three beam velocities to consider; that between the first and second cavity (which is independent of signal level) and those be-

Fig. 26 — *Power delivered to intermediate cavities*

21

tween second and third, and third and fourth cavities (which depend upon the powers delivered to the second and third cavities).

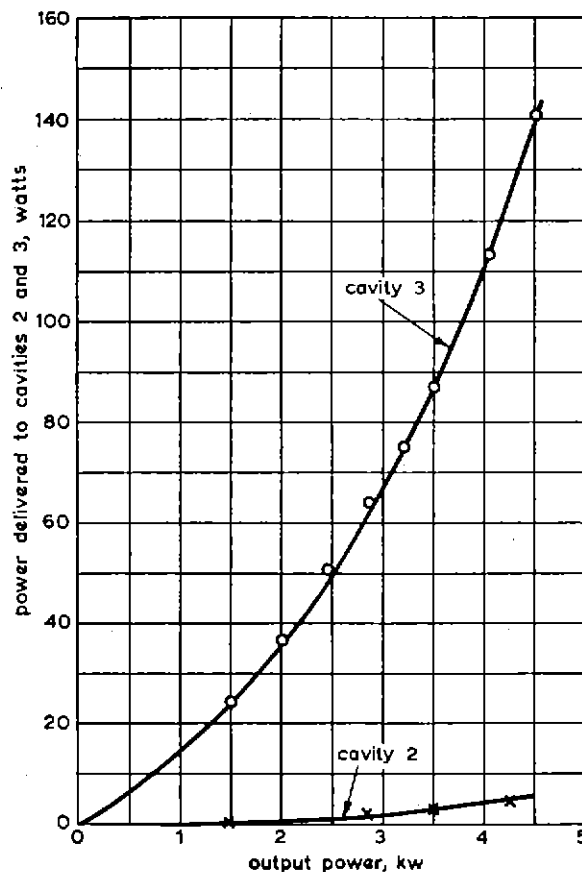The measured powers delivered to the second and third cavities have been shown in Fig. 9 and are re-plotted in Fig. 26 as a function of output power. It is evident that the power delivered to the second cavity is negligible compared to that delivered to the third cavity; only the change of velocity between the third and fourth cavity need therefore be considered.

If the length of the drift tube between the third and fourth cavities is l, the mean transit time of the beam along this tube is given by

$$T=\frac{l}{u_0}\left(1-\frac{P_{rf}}{P_0}\right)^{-\frac{1}{2}} \qquad (22)$$

where P_{rf} represents the power delivered to the third cavity. The change of transit time, compared to that when $P_{rf}=0$, is given by

$$\delta T=\frac{l}{u_0}\left[\left(1-\frac{P_{rf}}{P_0}\right)^{-\frac{1}{2}}-1\right] \qquad (23)$$

and, since P_{rf}/P_0 is small compared to unity, the change of phase of the output signal is given by

$$\delta\phi=\frac{\pi fl}{u_0}\cdot\frac{P_{rf}}{P_0} \qquad (24)$$

where f is the signal frequency.

Taking l as 120 mm, P_0 as 15·9 kW (see Section 3.1), and values of P_{rf} as shown in Fig. 26, the theoretical level-dependent phase shift as a function of output power at 675 MHz is as shown in Fig. 27. These results are evi-
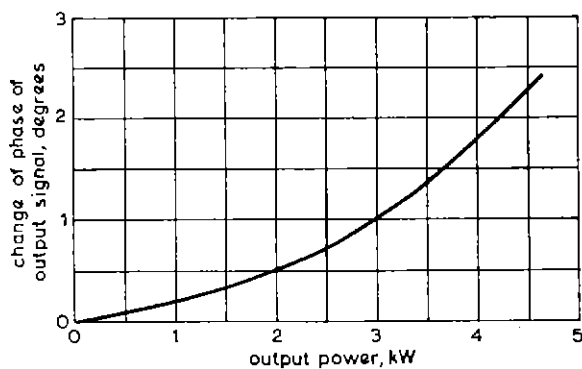
Fig. 27 — Theoretical level-dependent phase shift

dently of the same order as the measured results given in Section 3.7.

4.7 *Change of Phase of Output Signal with Beam Voltage*

It follows from Equation (1) that the transit time* through the klystron is given by

* This refers to the beam transit time. The envelope group delay through the klystron will be greater because of the phase characteristics of the cavities.

$$T=\frac{l}{\sqrt{(2\eta V_0)}} \qquad (25)$$

where l is the overall length of the drift tube from input to output cavities, and V is the beam voltage (cathode/body).

When the beam voltage is changed from V_1 to V_2, the change of phase of the output signal will be given by

$$\delta\phi=\pi fl\left[\frac{1}{\sqrt{V_1}}-\frac{1}{\sqrt{V_2}}\right]\cdot\left(\frac{2}{\eta}\right)^{\frac{1}{2}} \qquad (26)$$

Taking l as 370 mm, the theoretical phase change of an output signal at 675 MHz is shown as a function of beam voltage in Fig. 19. This result is in good agreement with the measured results.

5. Reverse Beam Current

As part of the klystron design, it is important to ensure that negligible reverse current (i.e. in the direction from collector to cathode) flows in the drift tube. Electrons which are deflected back from the collector for any reason would flow towards the body; such electrons would experience the same focusing action as do the forward electrons and would couple back from the output to the input cavity, giving rise to instability. The following describes two important ways in which reverse beam current can occur.

5.1 *Secondary Emission*

The electrons have sufficient velocity to cause secondary emission when they strike the collector; a few high-energy secondary electrons travel back along the drift tube. Measurements of back-coupling (from cavity 2 to cavity 1) have shown a reverse beam current to exist, probably caused in this way. It has been suggested that the presence of this reverse beam current can enhance the level of intermodulation products by introducing them back into the input cavity for re-amplification but it would seem that, even if the klystron were on the verge of self-oscillation due to the same cause, such enhancement cannot exceed 6 dB. Permanent magnets have been attached to the outer surface of the collector (by the klystron manufacturer) with a view to introducing a magnetic field which would deflect such secondary emission away from the drift tube.
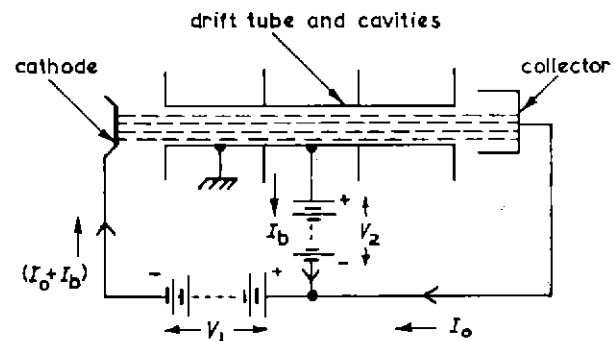
Fig. 28 — Depressed-collector operation

22

The manufacturer states that '. . . Fitting a magnet on the collector had the effect of stabilising the intermodulation product measure resulting in an improvement in some cases and a deterioration in others. One important feature of the magnet was that when present the intermodulation product followed the theoretical 2 dB per 1 dB law but in the absence of the magnet this law was generally not followed.'

5.2 *Depressed-collector Operation*

Electrons travel along the drift tube, and enter the collector, with a mean velocity largely determined by the cathode-to-body voltage. The energy which they possess after leaving the output cavity appears as heat on impact on the walls of the collector and is wasted. It would therefore appear desirable to depress the collector potential (i.e. make the collector potential negative with respect to the body) so as to slow down the electrons after leaving the output cavity but before impact on the cavity walls. A suitable arrangement would be that shown diagrammatically in Fig. 28. If $(V_1 + V_2)$ is made equal to V_0, the conditions throughout the drift tube and cavities are identical to those for normal operation (see Fig. 1). The electrons leaving the output cavity are decelerated by the voltage V_2 and, since the body current I_b is negligible compared to the beam current I_0, the d.c. power requirement is reduced from $V_0 I_0$ to $V_1 I_0$.

Such arrangements are quite practicable and are adopted on some commercially-available klystrons designed for u.h.f. television signals. It is desirable from the point of view of efficiency to make the ratio V_2/V_1 large but too large a value could lead to instability on account of the 'spread' of electron velocities about the mean value. This spread is small when the klystron is not driven but it increases as the level of input signal is increased. As the output power approaches the saturated power, some electrons leave the output cavity with comparatively low velocity and, if the ratio V_2/V_1 is sufficient, they may be turned back along the drift tube without touching the collector. The action becomes that of a reflex klystron and instability results. Nevertheless, a measure of collector depression is practicable. Four-cavity u.h.f. klystrons are commercially available for which $V_1 = 13$ kV and $V_2 = 5$ kV. The quoted saturation power of such klystrons is $58 \cdot 5$ per cent of the d.c. power, compared to only $31 \cdot 6$ per cent for the klystron used for the tests described in this monograph. In the authors' opinion, this is a very worthwhile advantage.

6. Envelope Correction

This section considers the possibility of pre-distorting the modulation envelope of the input signal to the klystron in such a manner that the envelope of the output signal is undistorted. Correction of this form could, in principle, remove all in-band intermodulation products. Two types of correction will be considered: open-loop methods which employ pre-set distorting networks, and closed-

loop methods in which the non-linear characteristics of the networks are adjusted by some feed-back mechanism.

6.1 *Open-loop Correction*

Open-loop correction requires a pre-distortion network, prior to the klystron,* which would generate intermodulation products with suitable amplitude and phase to cancel those generated subsequently in the klystron. This clearly pre-supposes highly stable non-linear characteristics of both the distorting network and the klystron. It also pre-supposes that the non-linearity/frequency characteristic of the network can be matched to that of the klystron; this may not be feasible because the non-linear characteristics of a stagger-tuned multi-cavity klystron would be highly frequency-dependent.

Such an approach is possible for first-order correction such as sync.-pulse stretching to allow for subsequent crushing in the klystron at a high-power station but it is considered to be quite impracticable as a method for reducing intermodulation products in a klystron when used as a common amplifier for sound and vision signals.

6.2 *Closed-loop Correction*

Closed-loop correction implies the use of a pre-distorting network whose non-linear characteristics are controlled by a signal which is derived from the envelope of the output signal. At first sight it would appear feasible to compare the envelopes of the signals at the input and the output of the klystron and to modulate their difference on to the input signal in cancelling phase. Simple loops of this type are not practicable, however, because the group delay through the klystron would limit their bandwidth to about 1 to 2 MHz. In order to apply closed-loop correction, therefore, it would be necessary to use a controlling signal, derived from the output signal, to re-adjust the non-linear characteristics of a pre-distorting network in such a way as to correct for changes in the characteristics of the klystron. It should be noted that, for envelope correction of this type, the controlling signal should be derived by comparing the envelope of the input signal with that of a portion of the output signal which has passed through a network having amplitude and phase characteristics similar to those of a typical domestic television receiver. The feasibility of this type of correction may be looked into in the future.

7. Conclusions

The principal assumptions in the theory of klystrons as given in this report have been to assume a two-cavity model and to neglect de-bunching. Both these assumptions are valid at low power levels but both would be expected to break down at output levels approaching the saturated power. Comparison between the measured and

* The network could equally, in principle, be connected at the output of the amplifier but such an arrangement would be less convenient in practice.

theoretical results has shown them to be in good agreement up to at least half the saturated power and to give a good estimate of the klystron performance at all power levels. The observed non-linearity of klystrons is therefore considered to be largely fundamental to their mode of operation and is not likely to be improved upon by attention to their design.

At main stations, where the sound and vision signals are handled by separate klystrons, it is possible to pre-distort the vision signal waveforms so as to overcome the effect of this non-linearity and the output power can approach the saturated power. Under these conditions, the peak efficiency is 30 to 40 per cent. At relay stations, however, where the klystrons are used as common amplifiers for both sound and vision signals, in-band intermodulation terms are generated which, at the present time, can only be made sufficiently small by restricting the peak output power to one-fifth of the klystron rated power. Used in that way, the peak efficiency is only about 6 per cent and, under average picture conditions, the mean efficiency is much less.

It is therefore evident that the low efficiencies at which klystrons are operated are partly fundamental to their mode of operation and partly determined by their non-linear characteristics. The efficiency can be increased by depressed-collector operation. This is a question of design but it would appear desirable, in association with klystron manufacturers, to determine the extent to which the design can be modified so as to permit the largest possible collector depression.

8. Acknowledgements

Thanks are due to Designs Department for their assistance during the measurements of differential amplitude and phase described in Sections 3.6 and 3.7, to Dr P. J. Joglekar who made the measurements described in Section 3.5.1, and to both the English Electric Valve Company and The M.E.L. Equipment Co. Ltd, for several helpful discussions as the work proceeded.

9. References

1. Webster, D. L., Cathode-ray Bunching, J. Appl. Phys., Vol. 10, pp. 501–8, July 1939.
2. Webber, S. E., Ballistic Analysis of a Two-cavity Finite Beam Klystron, I.R.E. Trans. Electronic Devices, pp. 98–108, April 1958.
3. Hahn, W. C., Small-signal Theory of Velocity-modulated Electron Beams, Gen. elect. Rev., Vol. 42, No. 6, pp. 258–70, 1939.
4. Hahn, W. C., Wave Energy and Transconductance of Velocity-modulated Electron Beams, Gen. elect. Rev., Vol. 42, No. 11, pp. 497–502, 1939.
5. Ramo, S., Space Charge and Field Waves in an Electron Beam, Phys. Rev., Vol. 56, pp. 276–83, August 1939.
6. Beck, A. W. H., Space-charge Waves, Oxford, Pergamon Press, 1958.
7. Sims, G. D., and Stephenson, I. M., Microwave Tubes and Semiconductor Devices, London, Blackie, 1963.
8. Murata, S., Intermodulation Produced by Double-cavity Klystron, Tech. J., Japan Broadcasting Corporation, Vol. 16, No. 5, pp. 1–8, 1964. (In Japanese.)
9. Curtice, W. R., Approximate Analytical Expression for Current Bunching in Three-cavity Klystron, Proc. I.E.E.E., Vol. 53, No. 11, pp. 1743–4, 1965.
10. Webber, S. E., Large Signal Analysis of the Multi-cavity Klystron, I.R.E. Trans. electronic Devices, pp. 306–15, October 1958.
11. Curnow, H. J., Factors Influencing the Design of Multi-cavity Klystrons. Proc. Instn. elect. Engrs., Vol. 105BS, No. 12, pp. 855–8, 1958.
12. O'Loughlin, C. N., Intermodulation Characteristics of High-power Klystrons used in Frequency Transposers for Colour Television, International Conference on UHF Television, London, November 1965. I.E.R.E. Conference Proceedings, 1965, No. 6, Paper No. 10.
13. Monteath, G. D., Whythe, D. J., and Hughes, K. W. T., Method of Amplitude and Phase Measurement in the VHF–UHF Band. Proc. Instn. elect. Engrs., Vol. 107B, No. 32, pp. 150–4, 1960.

10. Appendices

10.1 *The Ballistic Theory of Two-cavity Klystrons*

The mean velocity, u_0, with which electrons enter the input cavity is given by

$$e V_0 = \tfrac{1}{2} m \, u_0^2$$

or
$$u_0 = \sqrt{2\eta V_0} \qquad (27)$$

where V_0 is the cathode-to-body potential and η is the electron charge-to-mass ratio, $e/m (= 1 \cdot 759 \times 10^{11}$ coulomb/kg).

If the length of the drift-tube gap inside the input cavity is d, and the signal voltage across this gap is $V_1 \sin \omega t$, the acceleration experienced by an electron within the gap at time t will be given by

$$\frac{du}{dt} = \frac{\xi \eta V_1}{d} \sin \omega t \qquad (28)$$

where ξ is a gap coupling factor which depends upon the geometry of the gap and the electron beam. If the electron takes a small time, δt, to pass across this gap such that the 'transit angle' $\omega \delta t$ is small enough for $\sin \omega \delta t$ to be written as $\omega \delta t$ (i.e. the gap length d is a small fraction of the signal wavelength in the plasma) the acceleration of each electron can be regarded as uniform whilst in the gap and electrons can be regarded as leaving the input cavity at equal intervals of time but with differing velocities. Then, by the ordinary laws of kinematics, the velocity with which an electron leaves the gap at time t can be shown to be

$$u = u_0 [1 + \Delta \sin \omega t] \qquad (29)$$

where
$$\Delta = \frac{\xi V_1}{2 V_0}$$

If τ represents time measured at the output cavity, this electron travels along the drift tube with this velocity and arrives at the output cavity, distant z from the input cavity, at time $(\tau + \tau_0)$ given by

$$\tau + \tau_0 = t + \frac{z}{u_0(1 + \Delta \sin \omega t)} \tag{30}$$

Expanding by the binomial theorem, and dropping terms in Δ^2 and higher powers of Δ,

$$\tau + \tau_0 = t + z/u_0 - \frac{z\Delta}{u_0} \sin \omega t \tag{31}$$

The term z/u_0, representing the mean propagation time of the plasma, corresponds to a constant group delay (τ_0) which may be ignored. We therefore define

$$\tau = t - \frac{K}{\omega} \sin \omega t \tag{32}$$

where K is the 'bunching parameter' given by

$$K = \frac{\omega z \Delta}{u_0} \tag{33}$$

Let $I(\tau)$, the current passing through the output cavity, be expressed as a Fourier series. Since, for a sinusoidal input signal, it is an even function of τ,

$$I(\tau) = I_0 + \sum_{r=1}^{\infty} a_r \cos(r\omega\tau) \tag{34}$$

where

$$a_r = \frac{1}{2\pi} \int_{-\pi}^{+\pi} I(\tau) \cos(r\omega\tau) d(\omega\tau) \tag{35}$$

Before discussing the evaluation of the integral in Equation (35) it is necessary to mention three critical values of the bunching parameter K which is defined by Equation (33). Suppose Figs. 29(a) and 29(b) represent the flow of electrons in the vicinity of the output cavity, for two values of K. Each dot represents an electron; the equi-spaced dots in the upper half of each figure represent electrons leaving the input cavity at equal intervals of time whilst the unequally spaced dots in the lower half of each figure represent the same electrons arriving at the output cavity at unequal intervals of time. Each of the regions A, B, C, etc. contain the total charge emitted from the cathode during

successive r.f. periods. If $K < 1$, no electron overtaking occurs and electrons arrive at the output cavity in the same sequence that they left the input cavity. If $K > 1$, electron overtaking occurs and electrons arrive at the output cavity in a sequence different from that in which they left the input cavity but, nevertheless, provided $K < 4 \cdot 603$, the total charge contained in each of the regions A, B, C, etc. remains constant throughout the length of the drift tube. Since the klystron delivers its saturated power when $K = 1 \cdot 84$, the range of values of K for which this analysis is required fall well within the range $K < 4 \cdot 603$. Thus for all practical values of K, charge conservation applies over the range $-\pi < \omega\tau < \pi$ in the sense that all the electrons which pass the input cavity between successive zeros of the sinusoidal input signal (and no others) also pass the output cavity during the corresponding period. Thus

$$I(\tau)d\tau = I_0 dt \qquad \text{if } K < 1$$

but, if $1 < K < 4 \cdot 603$, two conditions apply; either

$$I(\tau)d\tau = I_0 dt \qquad \text{or} \qquad I(\tau)d\tau = I_0(dt_1 + dt_2 + dt_3)$$

where dt_1, dt_2 and dt_3 indicate the three time intervals at the input gap during which the current leaving the input cavity contributes to the current at the output cavity during the time interval $d\tau$. By the principle of charge conservation, the set of intervals dt covers a complete period. $I(\tau) d(\omega\tau)$ in Equation (35) may therefore be replaced by $I_0 d(\omega t)$ and, incorporating Equation (32) gives

$$a_r = \frac{I_0}{2\pi} \int_{-\pi}^{+\pi} \cos r\omega(t - \frac{K}{\omega} \sin \omega t) d(\omega t)$$

$$= 2I_0 J_r(rK) \tag{36}$$

and the complete harmonic series for the current passing the output cavity becomes

$$I = aI_0 \left[1 + 2 \sum_{r=1}^{\infty} J_r(rK) \cos r\omega t \right] \tag{37}$$
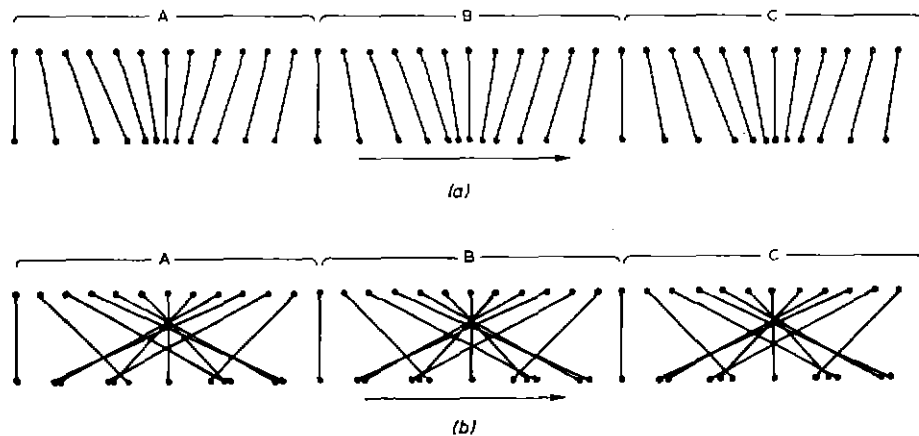

Fig. 29 — Times of arrival of electrons at the output cavity

where a is a constant which is proportional to the product of the input and output gap coupling factors.

It can be shown that the same result applies if $K > 4 \cdot 603$ but the proof is more involved and the question has no practical significance.

10.2 An Approximate Method of Estimating the Amplitude/Frequency Characteristic of a Rectangular Cavity*

Suppose the cavity is excited by a current I which passes through a central hole in its upper and lower faces. This type of excitation will give rise to TE fields in the cavity. Suppose the cavity to be split into two halves, each loaded with capacitance $C/2$ at its open end as shown in Fig. 30.
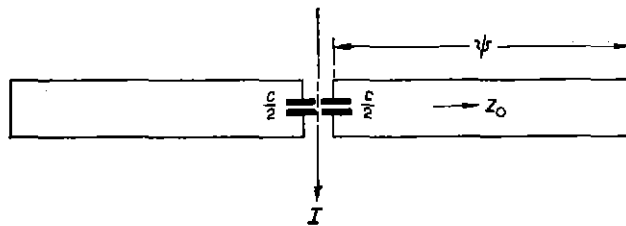

Fig. 30 — Cross-section through rectangular cavity with central capacitive loading

For the purpose of this approximate analysis, the cavity will be treated as two identical short-circuited transmission lines of electrical length ψ and characteristic impedance Z_0. The co-ordinate system to be adopted is shown in Fig. 31.
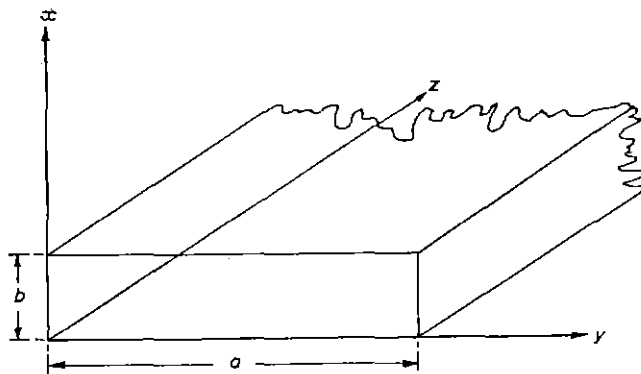

Fig. 31 — Co-ordinate system adopted for analysis of rectangular cavity

If the modulus of the voltage across the cavity is $|V|$, then, neglecting all losses,

$$|V| = \left| \frac{I}{2(B_{cav} + B_{cond})} \right| \qquad (38)$$

where

$$B_{cav} = \frac{\cot \psi}{Z_0} \qquad (39)$$

* This theoretical analysis was carried out by Mr L. K. Bradley.

and

$$B_{cond} = \frac{\omega C}{2} \qquad (40)$$

The wavelength in the cavity is given by

$$\frac{1}{\lambda_g^2} = \frac{1}{\lambda_0^2} - \frac{1}{4a^2}$$

where λ_0, the free-space wavelength, is given by

$$\lambda_0 = \frac{2\pi c}{\omega}$$

where c is the velocity of light.
Hence

$$\psi = \frac{\pi l}{a\lambda_0}(4a^2 - \lambda_0^2)^{\frac{1}{2}} \qquad (41)$$

where l is the length of each half of the cavity.

The characteristic impedance of the cavity is taken to be

$$Z_0 = \frac{\int_0^b E_x dx}{\int_0^a H_y dy}$$

$$= \frac{2b}{(4a^2 - \lambda_0^2)^{\frac{1}{2}}} \cdot \left(\frac{\mu}{\epsilon}\right)^{\frac{1}{2}} \qquad (42)$$

where μ and ϵ are the permeability and permittivity of the medium filling the cavity. For this case,

$$\mu = 1 \cdot 2566 \times 10^{-6} H/m$$

$$\epsilon = 8 \cdot 855 \times 10^{-12} F/m$$

and $\quad \sqrt{(\mu/\epsilon)} = 376 \cdot 7$ ohms

If the parameters a, b, l and C are known, the amplitude/frequency characteristic of the cavity can be calculated by determining the values of B_{cav} and B_{cond} as functions of frequency from Equations (39) to (42) and inserting them in Equation (38). In this case, the values of b and l were known but the values of a and C were not. The latter values were therefore deduced as follows.

It was found by experiment that, when the fundamental cavity resonance (i.e. the TE$_{011}$ mode) occurred at $674 \cdot 7$ MHz, the next resonance (i.e. the TE$_{013}$ mode) occurred at 1,346 MHz. This gives sufficient information to calculate a and C but the experiment was repeated using a different (but unknown) value for dimension a so that a confirmatory calculation could be made. With this new value, the TE$_{011}$ and TE$_{013}$ modes were found to occur at 630 MHz and $1312 \cdot 5$ MHz respectively.

With the known values of b and l, values of C were calculated for which TE$_{011}$ and TE$_{013}$ resonances would occur at the above four frequencies for various values of a. These are plotted in Fig. 32 as a function of a. The point of intersection of each TE$_{011}$ curve with its associated TE$_{013}$ curve gives the values of C and a which satisfy the
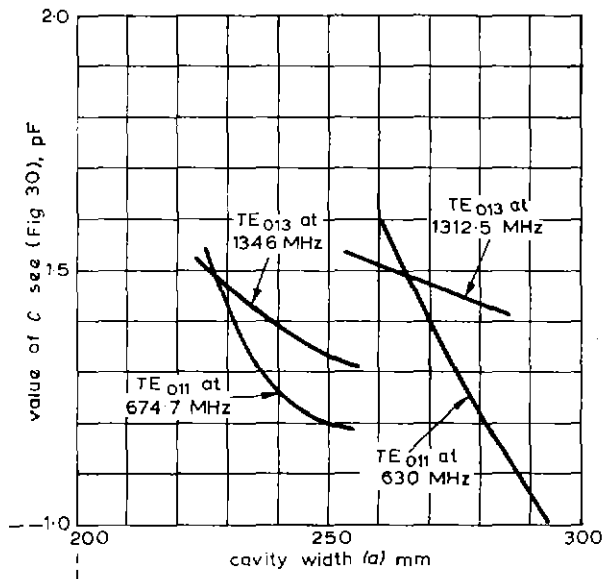
26

Fig. 32 — *Values of C giving first-order and third-order mode resonances at specified frequencies, as a function of cavity width*

two conditions. It will be observed from Fig. 32 that both sets of calculations agree that the value of C is about $1\cdot5$ pF.

The value of a which gives the TE_{011} resonance at any other desired frequency may now be readily determined and hence the associated overall amplitude/frequency characteristic calculated.